

Superdense Objects in General Relativity:  
Modeling Neutron Stars with Free Quark Cores

by

Joel C. Corbo

Submitted to the Department of Physics  
in partial fulfillment of the requirements for the degree of

Bachelor of Science

at the

MASSACHUSETTS INSTITUTE OF TECHNOLOGY

June 2004

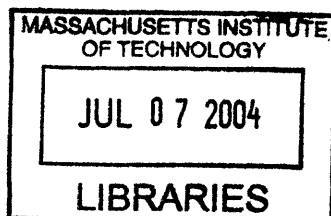
© Joel C. Corbo, MMIV. All rights reserved.

The author hereby grants to MIT permission to reproduce and  
distribute publicly paper and electronic copies of this thesis document  
in whole or in part.

Author .....  
Department of Physics  
May 7, 2004

Certified by .....  
Scott A. Hughes  
Assistant Professor  
Thesis Supervisor

Accepted by .....  
David E. Pritchard  
Senior Thesis Coordinator, Department of Physics



ARCHIVES



# Superdense Objects in General Relativity: Modeling Neutron Stars with Free Quark Cores

by

Joel C. Corbo

Submitted to the Department of Physics  
on May 7, 2004, in partial fulfillment of the  
requirements for the degree of  
Bachelor of Science

## Abstract

We present the results of a numerical study of neutron stars made of a color-flavor locked (CFL) quark matter center and a nuclear fluid exterior. CFL quark matter is a theoretical state of matter which may exist at the center of highly dense neutron stars. To verify its existence, we need to make falsifiable predictions about the differences between typical neutron stars and CFL hybrid neutron stars and verify them observationally. This thesis begins this process by modelling the hybrid neutron stars at rest and while undergoing rotation. We show that Newtonian models are insufficient to correctly describe these objects; their treatment must be relativistic. We also put a bound on the upper rotation speed allowed by our approximations. Finally, we note the presence of the backbending instability in our hybrid star model which may constrain the physically accessible parameters of this model. The tools we have developed in this study are a first step in fully investigating the properties of these objects.

Thesis Supervisor: Scott A. Hughes  
Title: Assistant Professor



## Acknowledgments

The author would like to thank Prof. Scott Hughes for being the best thesis advisor and graduate-school-application-process advisor ever! He would also like to thank Prof. Krishna Rajagopal for his insight into the theory behind CFL matter and for helping to discover the physics upon which this thesis fundamentally rests. Thanks also go to Prof. Mark Alford for providing the data upon which our fit to the hybrid neutron star equation of state is based.

Special thanks also goes to the author's parents, without whom he would not have had the encouragement and attention to make it as far as he has, to his floormates and other friends for constantly reminding him to "Work on your damn thesis!", and to Ink, the Panther, for being a source of much-needed 2AM amusement during the writing process.



# Contents

<b>1</b>	<b>Of Neutron Stars and Quarks</b>	<b>9</b>
1.1	Neutron Star Overview . . . . .	10
1.2	Neutron Fluid at High Density . . . . .	11
1.3	Some Idealizations . . . . .	13
<b>2</b>	<b>Static Neutron Star Models</b>	<b>17</b>
2.1	The Newtonian Equations of Hydrodynamics . . . . .	18
2.2	The Equation of State . . . . .	19
2.3	Interlude: Newton vs. Einstein . . . . .	22
2.4	Relativistic Changes to the Newtonian Model . . . . .	23
2.5	Numerical Results . . . . .	26
<b>3</b>	<b>Rotating Relativistic Models</b>	<b>31</b>
3.1	The Spacetime of a Static Star . . . . .	32
3.2	The Spacetime of a Rotating Star . . . . .	33
3.2.1	Spin Frequency and Angular Momentum . . . . .	36
3.2.2	Spherical Deformations . . . . .	38
3.2.3	Quadrupolar Deformations . . . . .	38
3.3	The Baryon Mass . . . . .	40
<b>4</b>	<b>Rotating Relativistic Results</b>	<b>41</b>
4.1	Verifying the Slow Spin Approximation . . . . .	41
4.2	Spin and Baryon Mass . . . . .	43

4.3	Eccentricity and Angular Momentum . . . . .	46
<b>5</b>	<b>Conclusions</b>	<b>49</b>
5.1	Where have we been? . . . . .	49
5.2	Where do we go from here? . . . . .	50
<b>A</b>	<b>On Units</b>	<b>53</b>
<b>B</b>	<b>The Lane-Emden Solution</b>	<b>55</b>
B.1	The Method . . . . .	55
B.1.1	Polytropic . . . . .	56
B.1.2	Linear . . . . .	59
B.1.3	Hybrid . . . . .	61
B.2	Implications . . . . .	63



# Chapter 1

## Of Neutron Stars and Quarks

Neutron stars are some of the densest objects in the known universe. Since their initial prediction in 1938\* and their observational discovery in 1968 [3], much has been uncovered about their basic properties and behavior. Recent work in QCD has revealed that there may be more to neutron stars than was previously understood. The theoretical prediction of a new phase of matter even denser than a fluid of neutrons has led to speculation that there may be neutron stars with this phase in their centers.

Unfortunately, there is currently no way to verify the existence of this new phase of matter in the laboratory; it seems that the only feasible way to experimentally discover it is to observe its effects on neutron stars. In order to do that, one must first make testable predictions about what measurable difference, if any, can be used to distinguish between ordinary neutron stars and the ones that contain this new type of matter. The purpose of this thesis is to start making useful predictions based on these new neutron star models and to compare these predictions to what is known about ordinary neutron stars.

To set the stage for this analysis, we will first discuss a bit both about neutron stars and about this new phase of matter.

---

\*Landau was the first person to publish a paper about neutron stars, although he theorized that they existed at the cores of stars and provided their energy [1]. It wasn't until the following year that Zwicky described the modern concept of neutron stars as stellar objects different from normal stars [2].

## 1.1 Neutron Star Overview

Neutron stars, along with white dwarfs and black holes, are members of a class of astrophysical objects called *compact objects*, which form in the death of stars.

In the absence of forces to provide outward pressure, any collection of massive particles in space, such as a planet or star, will collapse under the influence of gravity. Both planets and stars have a mechanism that provides the pressure they need to overcome gravitational collapse. In the case of a rocky planet like the Earth, this mechanism is obvious: the incompressibility of solid and liquid rock that arises from the chemical structure of these materials prevents the Earth from undergoing gravitational collapse. For a star like our sun, the outward pressure comes from the heat produced in the star's core as it undergoes nuclear fusion, converting hydrogen into helium and other heavier elements.

Eventually, a star will run out of nuclear fuel to burn, causing it to cool. The resulting loss of thermal pressure will allow the star to collapse until quantum mechanics steps in to counteract gravity. Once the density increases sufficiently, the electrons in the star will be pushed so close together that they will resist further compression simply due to the Pauli exclusion principle<sup>†</sup>. A star held up by this electron degeneracy pressure is called a *white dwarf*. White dwarfs are typically about the same size as the Earth and are very common in the universe, as they are the end state for most stars [4].

For stars with mass higher than a certain cutoff, called the Chandrasekhar limit, electron degeneracy pressure is not enough to prevent further gravitational collapse. The Chandrasekhar limit is about  $1.4 M_{\odot}$ , where  $M_{\odot} = 1.99 \times 10^{33}$  g is the mass of the sun [5]. Above this mass, gravity will force the electrons in the star to come so close together that they will be forced to combine with protons through inverse beta decay, creating neutrons and neutrinos. The neutrinos escape, leaving behind a

---

<sup>†</sup>The Pauli exclusion principle states that no two fermions can occupy the same quantum state at the same time. This means that there is a limit to how much a group of fermions like electrons can be compressed before degeneracy pressure prevents further compression. Compare this to the behavior of a group of bosons, like the photon. Because bosons do not obey the exclusion principle, an arbitrary number of them can occupy the same state, so they do not resist compression into a small volume.

*neutron star*, a star made entirely of neutrons<sup>†</sup> and held up by the neutron degeneracy pressure caused by the exclusion principle. Neutron stars have a typical radius of 10 km [5].

If the mass of the original star is greater still, even neutron degeneracy pressure will not be able to hold it up against gravitational collapse. Above a new mass cutoff, the Oppenheimer-Volkoff limit of about 3-4  $M_{\odot}$ <sup>§</sup>, nothing can prevent the star from collapsing into a black hole, the end of the line when it comes to gravitational collapse [5].

## 1.2 Neutron Fluid at High Density

Until recently, it was generally believed that the previous section summarized the entire story for compact objects. Without some material that exists at even higher densities than a fluid of neutrons, there can be no object both denser than a typical neutron star and stable against collapse into a black hole. As it turns out, recent work in QCD has brought forth a likely candidate for such a material: a type of quark matter called the color-flavor locked (CFL) phase. The detailed theory of this new phase of matter is beyond the scope of this thesis. Here, we will attempt to paint a general picture of the properties of the CFL phase. We follow the presentation found in [6] throughout this section.

The CFL phase is the ground state for QCD at asymptotically high densities with only up, down, and strange quarks present. In the CFL phase, the quarks form  $ud$ ,  $us$ , and  $ds$  Cooper pairs, with a pairing energy associated with each type of pair. The pairing energy is the amount by which each Cooper pair lowers the overall energy of the quark fluid and is maximized when there is an equal number density of  $u$ ,  $d$ , and  $s$ . Because of this, the CFL phase consists of equal numbers of  $u$ ,  $d$ , and  $s$ ,

---

<sup>†</sup>This is actually only true to first approximation. In fact, the fluid of a neutron star consists of neutrons in beta decay equilibrium with a very small fraction of protons and electrons.

<sup>§</sup>The Oppenheimer-Volkoff limit is dependent on the exact relationship between the density and pressure of a neutron star, which is currently not understood well enough to pin down its value better than the range here stated.

and is therefore electrically neutral<sup>¶</sup>. This is important because macroscopic bulk matter should, in general, be electrically neutral. It is also quite different than the situation for non-CFL quark matter. Because the strange quark has a much higher mass than the up or the down quark, an unpaired fluid of quarks will have a much higher number density of up and down quarks than strange quarks. This leads to a net positive charge which is neutralized by the presence of electrons. Because CFL matter has equal numbers of these three quarks, there is no net charge to cancel and therefore no electrons.

The CFL phase breaks the color and electromagnetic gauge symmetries, meaning, among other things, that ordinary photons cannot exist in such matter. However, one can show that there is an unbroken U(1) gauge symmetry similar to the U(1) symmetry associated with electromagnetism. This symmetry gives rise to a new “rotated” photon which is a linear combination of an ordinary photon and one of the eight gluons. The CFL phase is neutral with respect to this new symmetry, which allows the rotated photon to pass right through it. Additionally, at temperatures sufficiently lower than its Fermi temperature, the CFL phase becomes a superfluid. Any neutron star more than a few seconds old will have cooled enough to meet this condition. Therefore, any CFL matter existing at neutron star temperatures and densities would be a transparent superfluid.

The existence of this new type of matter leads to new possibilities for compact objects. It implies that there should be some new mass threshold below which one finds neutron stars made entirely of nuclear matter and above which one finds “hybrid” neutron stars with CFL phase interiors surrounded by nuclear matter. The transition at the interface between CFL matter and nuclear matter involves very interesting physics. For a sharp boundary of about 10 fm, the difference in chemical potentials between the CFL and nuclear sides will cause electrons to flow out of the nuclear matter into the CFL matter. This leads to a buildup of protons on the nuclear side, which in turn leads to a buildup of negative kaons on the CFL side, all in the right densities

---

<sup>¶</sup>The charge of the up quark is  $2/3$  of the fundamental charge  $e$ , while the charge of both the down and strange quarks is  $-1/3e$ .

to balance the resulting electric field. If there is a mixed-phase region instead of a sharp interface, things become even more complicated. Preliminary analysis seems to indicate that the sharp boundary is the more likely to occur in nature.

For our purposes, a detailed description of CFL matter is not important. As we will see, in order to model a neutron star all that is really necessary is the *equation of state* of the matter making up the star, an equation that describes the relationship between pressure and mass density in the star. We will take the equation of state as a given in the next chapter. It is worth noting that the equation of state we chose assumes the model with the sharp interface rather than the mixed-phase transition.

### 1.3 Some Idealizations

Several idealizations are made in the treatment of neutron stars presented here. First, we assume that the nuclear matter in the neutron star has zero viscosity. For a static neutron star, this assumption clearly makes no difference. However, for a rotating neutron star it forces us to treat all of the nuclear matter in the star as corotating. This is a very useful simplification because it is much easier to model a body with the same angular frequency throughout its volume. Because CFL matter and the neutron fluid have the properties of a superfluid<sup>||</sup>, this idealization is justified.

The second idealization we make is to ignore the crust of the neutron star. To first approximation, the matter in a neutron star can be thought of as made entirely of neutrons. In reality this material is dominated by neutrons in beta-decay equilibrium with a small number of protons and electrons. Since higher pressure favors neutrons over proton-electron pairs, the fraction of neutrons decreases near the surface of the star until the nuclear fluid forms a crystalline crust layer. This crust is usually a few hundred meters thick and contains only a few percent of the total mass of the neutron star [5]. Because we are only concerned with global properties of the hybrid neutron stars, and because these hybrid neutron stars are very centrally condensed

---

<sup>||</sup>Actually, the neutron fluid ceases to be a superfluid near the surface. As we will discuss in the next paragraph, it is OK to ignore this because most of the mass of the star is away from the surface and therefore in a superfluid state

so that most of their mass lives in their small CFL centers, the presence of their crust is negligible and can be ignored.

The final idealization we make is to assume that the neutron stars we are modelling have zero magnetic field. Strictly speaking, we believe that this is never true because all neutron stars ever seen in nature have magnetic fields. However, if the magnetic field present is small enough, it will negligibly impact the fluid structure of the star. We can then treat it as being zero. A quick calculation will show what “small enough” means.

Magnetic fields have a magnetic energy density of the form

$$u_B = \frac{|\vec{B}|^2}{8\pi}, \quad (1.1)$$

in cgs units. Furthermore, we know from basic electromagnetism that electromagnetic energy densities give rise to pressures. For example, the magnetic pressure in the  $i$ -direction is given by the  $i$ - $i$  component of the Maxwell stress tensor. For  $E=0$ ,

$$P^i = T^{ii} = \frac{1}{8\pi} \left( 2B_i^2 - \vec{B}^2 \right), \quad (1.2)$$

which is approximately equal to the magnetic energy density

$$P_B \approx u_B. \quad (1.3)$$

Of course, a neutron star also has neutron degeneracy pressure holding it up. For the hybrid neutron stars of interest, the degeneracy pressure at the center of the star has a minimum value on the order of  $10^{34}$  dynes/cm<sup>2</sup>. The pressure in the star does fall off with distance from the center, but in such a way that all but about the outer 1 percent of stellar material is at a pressure between  $10^{34}$  and  $10^{32}$  dynes/cm<sup>2</sup> for the minimum central density. Taking  $10^{32}$  dynes/cm<sup>2</sup> as the lowest possible degeneracy pressure of interest, we estimate the magnetic field strength needed to produce a comparable magnetic pressure to be about  $5 \times 10^{16}$  Gauss. As it turns out, most neutron stars have an observed magnetic field of order  $10^{12}$  Gauss, although a handful, the so-called

*magnetars* [7, 8], have observed fields that are much higher. Also, since we do not know anything about a neutron star's internal field, it could be that it is much higher than the external field, although that is unlikely. Ignoring these possibilities, we find that the pressure due to the typical external magnetic field, which goes like the field squared, is 8 orders of magnitude smaller than the lowest degeneracy pressure that we care about. Thus, for our purposes, we can safely set the magnetic field to zero; its contribution to the overall pressure of the star is far less than the star's degeneracy pressure.





## Chapter 2

# Static Neutron Star Models

To first approximation, a neutron star is simple to describe mathematically. When static, a neutron star can be thought of as a spherically symmetric massive object characterized by its radius and its density, pressure and mass profiles. The relationships among these quantities are quite simple in the Newtonian limit, and methods have been developed over time to facilitate their calculation for typical neutron stars. Describing these methods and their application to hybrid neutron stars will be the subject of the first half of this chapter.

As we shall see, Newtonian gravity does not do an adequate job of describing the hybrid neutron stars. Neutron stars are very dense objects; because of this, general relativity plays an important role in determining their characteristics. For typical neutron stars, relativistic effects act as a fairly small correction\* as far as their masses and radii are concerned. This is not the case for hybrid neutron stars. Because they are so centrally condensed, the analysis of hybrid neutron stars requires a fully relativistic treatment, which we give in the latter half of this chapter. We will defer presentation of the numerical results for both the Newtonian and relativistic models until the end.

---

\*Here “small correction” means on the order of a few tens of percent. This may seem high, but given the amount of error associated with observing neutron stars from Earth, it can be a reasonable amount of uncertainty.

## 2.1 The Newtonian Equations of Hydrodynamics

With Newtonian gravity, the equations that describe the interior of a neutron star (or any other star, for that matter) are called the Newtonian equations of hydrodynamics, also known as the equations of stellar structure. For spherical stars, these equations are a set of first-order differential equations relating the mass, density, and pressure of a star as a function of radius:

$$\frac{dm}{dr} = 4\pi\rho r^2, \quad (2.1)$$

and

$$\frac{dP}{dr} = -\frac{Gm\rho}{r^2}, \quad (2.2)$$

where  $G$  is Newton's constant,  $6.67 \times 10^{-8}$  dynes-cm<sup>2</sup>/g<sup>2</sup>.

It is easy to derive the equations of stellar structure. Take a sphere of mass  $m$  and radius  $r$  whose density is a function of  $r$  only and imagine adding a thin layer of mass onto the sphere of thickness  $dr$ . The volume of this thin shell is

$$dV = 4\pi r^2 dr. \quad (2.3)$$

Because the shell has a uniform density  $\rho$ , the mass of the shell is

$$dm = 4\pi\rho r^2 dr, \quad (2.4)$$

which leads directly to Eq. (2.1).

Eq. (2.2) describes the gravitational attraction between the mass in the shell and the mass interior to the shell. The differential force on the shell is given by

$$dF = -\frac{Gmdm}{r^2}, \quad (2.5)$$

where  $dm$  is given by Eq. (2.4). Because we are interested in the force per unit area (that is, the pressure) on the shell, we divide by the surface area of the shell,  $4\pi r^2$ ,

to produce

$$\frac{dF}{A} = dP = -\frac{Gm\rho dr}{r^2}. \quad (2.6)$$

This leads directly to Eq. (2.2).

## 2.2 The Equation of State

The equations of stellar structure are not enough to completely describe a neutron star. By inspection, we can see that there is a function, the density  $\rho(r)$ , that is completely unspecified; as far as the equations are concerned,  $\rho(r)$  could equal anything! Of course, we know that the density is related to the pressure in some fashion, so we need to find a way to tell the equations of stellar structure just how they are related. This information is contained in the star's equation of state, usually written in the form  $P=P(\rho)$ <sup>†</sup>. By solving for  $\rho$  and plugging it into Eqs. (2.1) and (2.2), we get a set of differential equations for mass and pressure only, which is a completely determined problem given a set of initial conditions.

In some sense then, the equation of state is the thing that distinguishes one type of star from another; since all non-rotating fluid bodies obey the same equations of stellar structure, they are, on their own, not useful for understanding any particular type of star. On the other hand, once we know the equation of state for a particular body, all of its specific characteristics can be determined. Typical neutron stars can be fairly well approximated by a *polytropic* equation of state [5]:

$$P = k\rho^\Gamma. \quad (2.7)$$

Qualitatively, the  $\Gamma$  factor in Eq. (2.7) has interesting physical significance. The exponent  $\Gamma$  is a measure of the compressibility of the material making up the neutron star. For small  $\Gamma$ , the pressure changes very little when the density of the matter

---

<sup>†</sup>Actually, the equation of state is typically written as a function of density and entropy  $S$ . However, the temperature of neutron stars is sufficiently small compared to the Fermi temperature of a degenerate nuclear fluid that neutron stars can be well approximated as having zero entropy, eliminating  $S$  from the picture.

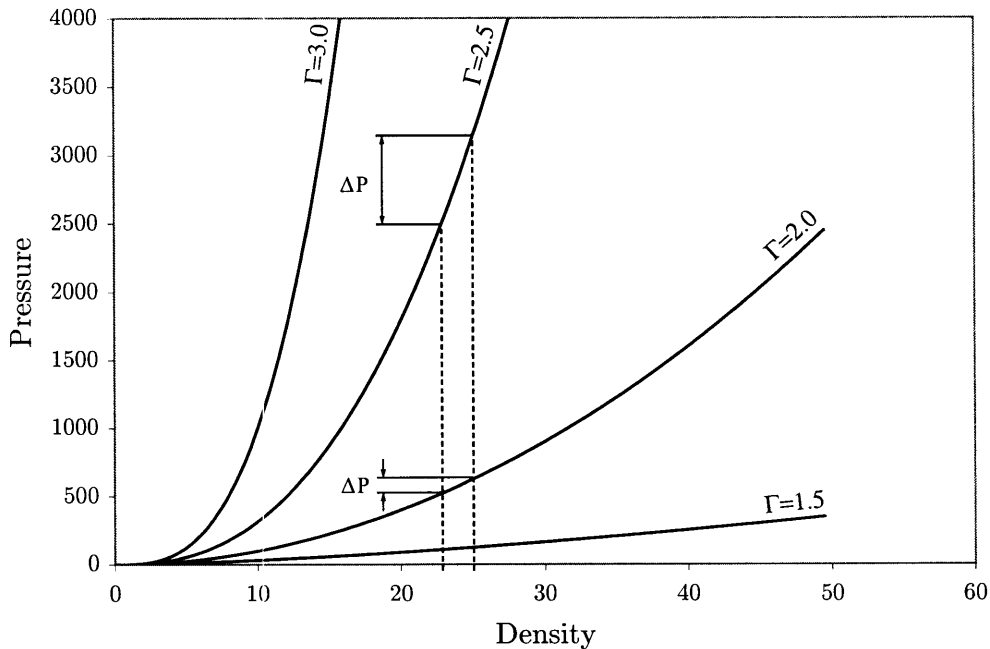


Figure 2-1: Examples of polytropic equations of state with  $k=1$  and  $\Gamma$  ranging from 1.5 to 3.0. For the same change in density, an equation of state with a higher  $\Gamma$  produces a higher change in pressure, making it less compressible.

making up the star changes. This means that the star is compressible, because it is possible to pack the same amount of matter into smaller volumes without an appreciable increase in the outward pressure to stop the compression. Stars like this will tend to be centrally-condensed. On the other hand, for stars with very large  $\Gamma$ , even a small increase in density due to compression will create a large increase in pressure to resist that compression. This will lead to an incompressible, more homogeneous star. See Fig. 2-1 for an example.

The neutron star of interest in this paper, namely one with a CFL matter center surrounded by a nuclear matter shell, has an equation of state that is best described by a hybrid of the polytropic equation of state and a “linear” equation of state:

$$\rho = \begin{cases} \left(\frac{P}{k}\right)^{1/\Gamma}, & P < P_T \\ \rho_{CFL} + \frac{P-P_T}{v_{CFL}^2}, & P > P_T \end{cases} \quad (2.8)$$

This equation is linear above some critical pressure  $P_T$  and polytropic otherwise; see

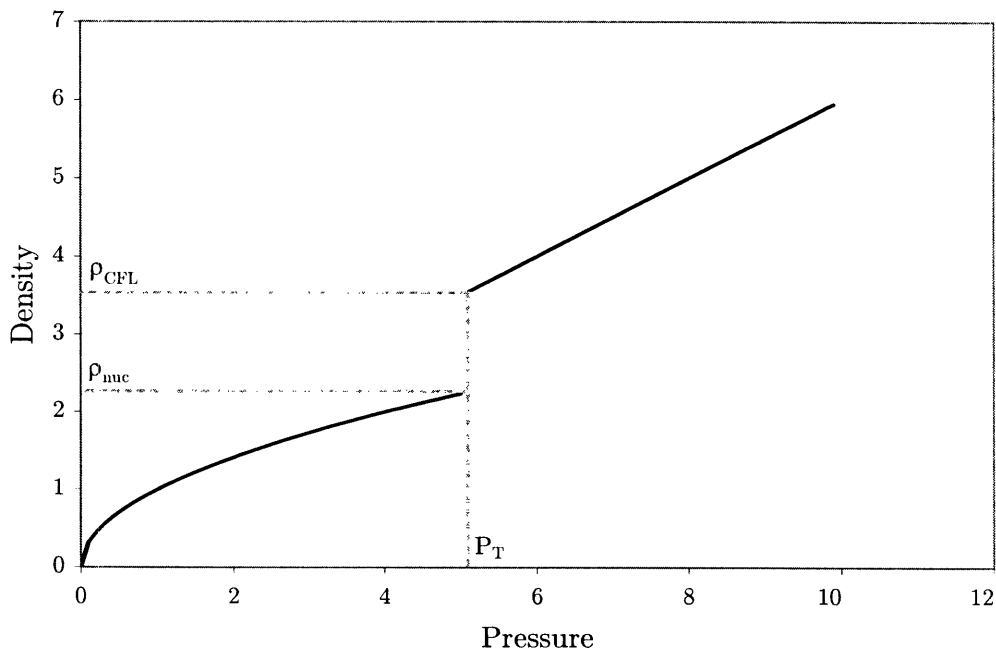


Figure 2-2: The hybrid equation of state, Eq. (2.8). The transition pressure  $P_T$  and the two transition densities  $\rho_{CFL}$  and  $\rho_{nuc}$  are indicated. Note that the axis of this plot have been exchanged compared to those in Fig. 2-1.

Fig. 2-2. The linear region of the plot characterizes the CFL matter in the central part of the star while the polytropic region characterizes the star's outer nuclear matter. One interesting fact to note is that there is a discontinuity in the density of the star at the transition from CFL to nuclear matter; the transitional CFL density  $\rho_{CFL}$  is roughly twice the transitional nuclear density  $\rho_{nuc}$ . Any densities between these two values are inaccessible<sup>†</sup>. Because the linear region has  $\Gamma=1$  while the polytropic region has  $\Gamma>1$ , we also know that the linear part of the star should be more condensed than the polytropic part. These statements together imply that the density of the central CFL matter is significantly higher than the density of the outer nuclear matter.

The linear part of Eq. (2.8) includes a parameter  $v_{CFL}$  that has the dimension of a velocity. If we take the derivative of  $P$  with respect to  $\rho$  in the CFL region of the equation of state, we find that it equals  $v_{CFL}^2$ . As it happens,  $dP/d\rho$  is proportional

<sup>†</sup>This discontinuity can only be discovered by doing the detailed QCD calculations hinted at in Chapter 1 of this paper. It is not a fundamental feature of the hybrid equation of state as its parameters could easily be tweaked to make the function continuous.

to the speed of sound squared in a material, so  $v_{CFL}$  is a measure of the speed of sound in the CFL region of the star.

It is also interesting to note one of the other implications of the hybrid equation of state: there can be no hybrid neutron star with only a CFL matter part. No matter what its central pressure, the pressure of the hybrid star at its boundary with space must be zero because pressure is always continuous. Therefore, if the central pressure is high enough to create CFL matter, there must necessarily be some radius at which the pressure in the star equals  $P_T$ , and there must therefore be a transition to nuclear matter. The CFL matter, if it exists, will stay hidden inside the neutron star.

Now that we know the equation of state for the hybrid neutron star, it is straightforward to numerically solve the equations of stellar structure<sup>§</sup>. Because we have two first-order coupled differential equations to solve, we will need to specify two quantities at the center of the star in order to produce a specific solution. We will choose to specify the mass and pressure:

$$m(r = 0) = 0 \tag{2.9}$$

$$P(r = 0) = P_{central}. \tag{2.10}$$

Given these, the integration of the equations can continue until  $P=\rho=0$ , which signals the surface of the star.

## 2.3 Interlude: Newton vs. Einstein

While the Newtonian model just discussed is a decent approximation for ordinary neutron stars, it fails to accurately model the hybrid neutron stars of interest. While the numerical results that support that statement will appear at the end of this chapter, it is not hard to believe that this claim is true based on some qualitative arguments.

---

<sup>§</sup>For the polytropic equation of state, one typical method for solving the equations of stellar structure involves putting them into a dimension-free form so that different stars can be related by simple scaling. It is possible to apply this method to the hybrid equation of state as well. See Appendix B for a full discussion.

For ordinary neutron stars, Newtonian models are accurate to a few tens of percent. We know that the central CFL region of the hybrid neutron stars are at least a factor of two more dense than normal nuclear matter, which implies that relativistic effects should be more important for the hybrid star than for a typical neutron star. Therefore, because hybrid neutron stars are so centrally condensed, they are best modelled using general relativity.

From a calculational perspective, the effect of GR is to modify the equations of stellar structure and to introduce a new type of mass density. At the end of the day, the numerical calculations needed to solve for the properties of hybrid neutron stars are no more difficult than those for the Newtonian model.

## 2.4 Relativistic Changes to the Newtonian Model

Several changes need to be made to the Newtonian equations of stellar structure and to the equation of state of a neutron star in order to correct them for relativistic effects. These changes are grounded in one major principle of general relativity: both matter and energy gravitate. This means that not only does the matter in a neutron star produce gravitational forces, but that the gravitational potential energy due to the matter itself is a source of gravity.

From a physical standpoint, this means that we need to define two types of mass density: the rest mass density  $\rho_0$  and the gravitational mass density  $\rho$ . The rest mass density of a neutron star, sometimes called the baryon mass density, is the mass density due to the rest masses of the neutrons making up the neutron star; it can be thought of as the product of the number density of neutrons with the rest mass of a single neutron. This is conceptually the same as the Newtonian mass density of the last chapter. In contrast, the gravitational mass density of a neutron star is the mass density one would infer by observing the orbit of a test mass around the neutron star. It includes the rest mass density in addition to terms that arise because of the gravitational field produced by the neutron star's binding energy [5].

This distinction between  $\rho$  and  $\rho_0$  changes the equations that describe neutron

stars. The equation of state remains a function of the rest mass density

$$P = P(\rho_0), \quad (2.11)$$

while Eq. (2.1) becomes a function of gravitational mass density

$$\frac{dm}{dr} = 4\pi\rho r^2. \quad (2.12)$$

The other equation of stellar structure changes in a more drastic way:

$$\begin{aligned} \frac{dP}{dr} &= \frac{-(\rho c^2 + P)(Gmc^2 + 4\pi r^3 GP)}{rc^2(rc^2 - 2Gm)} \\ &= \frac{-(\rho + P)(m + 4\pi r^3 P)}{r(r - 2m)}. \end{aligned} \quad (2.13)$$

We have followed the standard practice in general relativity of setting  $G=c=1$  in the second line. Eq. (2.13) is known as the Tolman-Oppenheimer-Volkoff equation. It is simple to derive exactly from the Einstein field equations for the case of spherical symmetry [9]; its form can be understood more physically [4]. Because both mass and energy contribute to gravitational fields, mass densities and energy densities are treated symmetrically in relativistic equations, and energy densities give rise to pressures. This explains the presence of the two pressure terms in the numerator. The extra mass term in the denominator arises from the fact that spacetime is curved around the neutron star, which introduces a factor when converting between the proper radius and the coordinate radius.

Because we have introduced a second type of density, we need yet another relationship to solve the equations of stellar structure: the relationship between  $\rho$  and  $\rho_0$ . In differential form, the desired relation is [5]

$$d\left(\frac{\rho}{\rho_0}\right) = -\frac{P}{c^2}d\left(\frac{1}{\rho_0}\right), \quad (2.14)$$



which comes from evaluating the first law of thermodynamics

$$dU = -PdV. \quad (2.15)$$

For the polytrope, we know

$$\frac{1}{\rho_0} = \left(\frac{k}{P}\right)^{1/\Gamma}, \quad (2.16)$$

which implies

$$d\left(\frac{1}{\rho_0}\right) = -\frac{k^{1/\Gamma}}{\Gamma} \frac{dP}{P^{1/\Gamma+1}}. \quad (2.17)$$

Substituting this into Eq. (2.14) and integrating both sides, we find

$$\begin{aligned} \frac{\rho}{\rho_0} &= \frac{k^{1/\Gamma}}{c^2\Gamma} \frac{P^{1-1/\Gamma}}{1-1/\Gamma} + C \\ &= \frac{1}{c^2(\Gamma-1)} \frac{P}{\rho_0} + C, \end{aligned} \quad (2.18)$$

where  $C$  is a constant of integration. We can then solve for  $\rho$

$$\rho = \frac{P}{c^2(\Gamma-1)} + C\rho_0. \quad (2.19)$$

To solve for  $C$ , we note that in the Newtonian limit of  $P \ll \rho_0 c^2$ , we expect that  $\rho \approx \rho_0$ . Therefore,  $C=1$  and

$$\rho = \rho_0 + \frac{P}{c^2(\Gamma-1)}. \quad (2.20)$$

For the linear equation of state, we follow a similar process. We note that

$$\frac{1}{\rho_0} = \frac{1}{\rho_{CFL} + (P - P_T)/v_{CFL}^2}, \quad (2.21)$$

which implies

$$d\left(\frac{1}{\rho_0}\right) = \frac{-dP}{v_{CFL}^2[\rho_{CFL} + (P - P_T)/v_{CFL}^2]^2}. \quad (2.22)$$

Again substituting into Eq. (2.14) and integrating, we find

$$\rho = \left(\frac{v_{CFL}}{c}\right)^2 \rho_{CFL} + \left(\frac{v_{CFL}}{c}\right)^2 \rho_0 \ln \rho_0 + C\rho_0. \quad (2.23)$$

Again taking the  $P \ll \rho c^2$  limit, we should find that  $\rho \approx \rho_0 \approx \rho_{CFL}$ . Solving for  $C$  in this limit, we find

$$C = 1 - \left(\frac{v_{CFL}}{c}\right)^2 - \left(\frac{v_{CFL}}{c}\right)^2 \ln \rho_{CFL}, \quad (2.24)$$

which, when substituted into the previous equation, gives

$$\rho = \rho_0 + \left(\frac{v_{CFL}}{c}\right)^2 \left[ \rho_{CFL} - \rho_0 + \rho_0 \ln \left( \frac{\rho_0}{\rho_{CFL}} \right) \right]. \quad (2.25)$$

Given the relationship between  $\rho$  and  $\rho_0$  for both the linear and the polytropic case, it is again possible to solve the equations of stellar structure directly as in the Newtonian case. The same conditions at the center of the star and at the surface apply.

## 2.5 Numerical Results

Fig. 2-3 is a plot of our fit to the hybrid equation of state produced by a QCD calculation. Based on this fit, we can find numerical values for the equation of state parameters that we are interested in. We find<sup>¶</sup>  $P_T = 5.234 \times 10^{34}$  dynes/cm<sup>2</sup>,  $\rho_{CFL} = 1.062 \times 10^{15}$  g/cm<sup>3</sup>,  $\rho_{nuc} = 5.596 \times 10^{14}$  g/cm<sup>3</sup>,  $v_{CFL} = 2.128 \times 10^{10}$  cm/s,  $k = 7.935 \times 10^{-6}$  (dynes/cm<sup>2</sup>).(g/cm<sup>3</sup>)<sup>-5/3</sup>, and  $\Gamma = 2.7$ . Note two interesting points about these values. First, the characteristic velocity for the CFL region is about 2/3 of the speed of light, which strengthens our argument that relativity should be important to our analysis. Second, the high value of  $\Gamma$  suggests that the nuclear region in a star with this equation of state is much less compressible than the CFL region. Both of these results confirm assertions we made in earlier parts of this chapter.

Perhaps the single most important result of our analysis of the static hybrid neutron stars is included in Fig. 2-4, which shows a plot of the mass of a Newtonian and a relativistic hybrid star as a function of its central pressure. While the Newtonian curve is much higher than the relativistic one, they share similar features. Both

---

<sup>¶</sup>Note that we have converted from nuclear physics units to cgs. See Appendix A for a discussion of units and conversions between them.

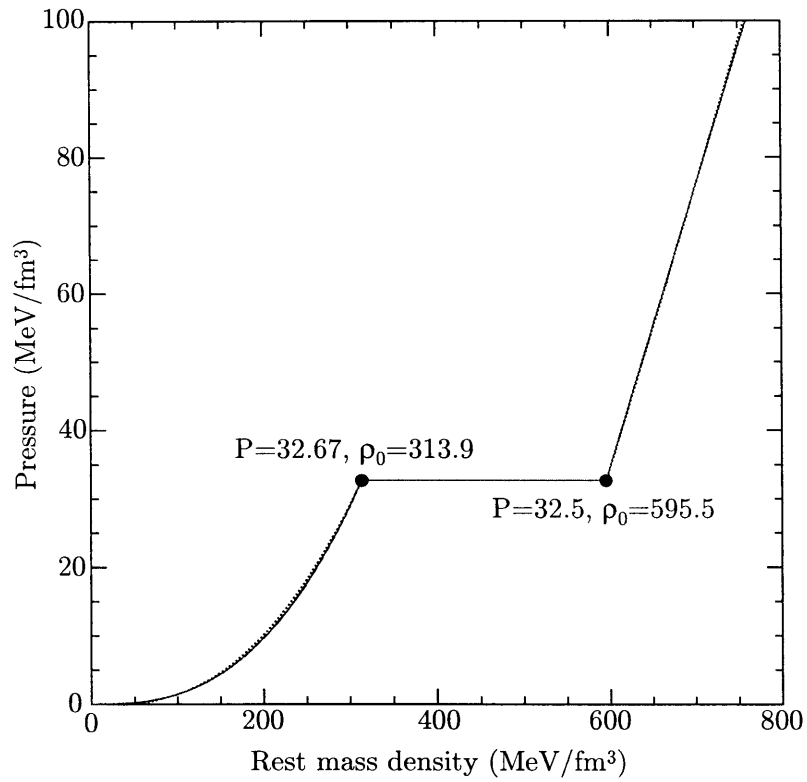


Figure 2-3: A fit to the hybrid equation of state from [10]. The solid line is the original data, provided by Mark Alford [11], while the dotted line is the fit. The units used are typical nuclear physics units; see Appendix A for a discussion of how to convert them to cgs and natural units.

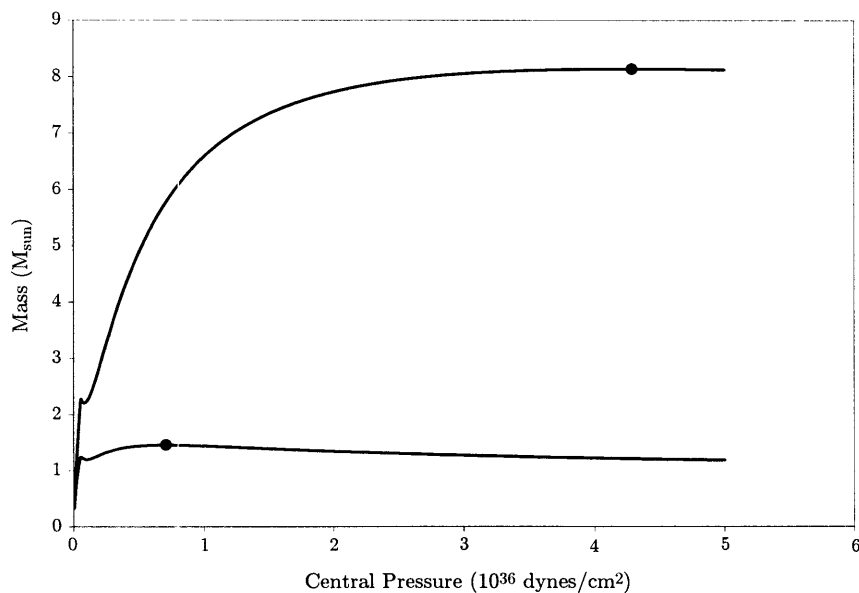


Figure 2-4: Mass vs. central pressure for a Newtonian hybrid star (upper curve) and a relativistic hybrid star (lower curve). The maximum in each curve is noted by a dot.

curves have maximum values, indicated by the dot on each curve; for the Newtonian model, the maximum mass of a star is  $8.14 M_{\odot}$  while for the relativistic model it is  $1.46 M_{\odot}$ . This is a huge discrepancy, and is the single biggest piece of evidence pointing at the inadequacy of the Newtonian model for the hybrid neutron stars. If relativity were just a small effect, then we would expect the maximum mass predicted by the relativistic model to be fairly close to the maximum mass predicted by the Newtonian model. Since they are enormously different, relativistic effects must be very important, and the Newtonian model cannot be trusted.

One other interesting result comes out of Fig. 2-4. For all stars to the left of the maximum in the relativistic model, the positive slope of the curve indicates that increasing the central pressure, and therefore central density, of a star increases its mass; this is a sensible result. However, on the other side of the maximum the slope of the curve changes sign. In that region, increasing the central pressure leads to a star with less mass, which does not make physical sense. What this means is that stars to the right of the maximum are highly unstable. If one did happen to

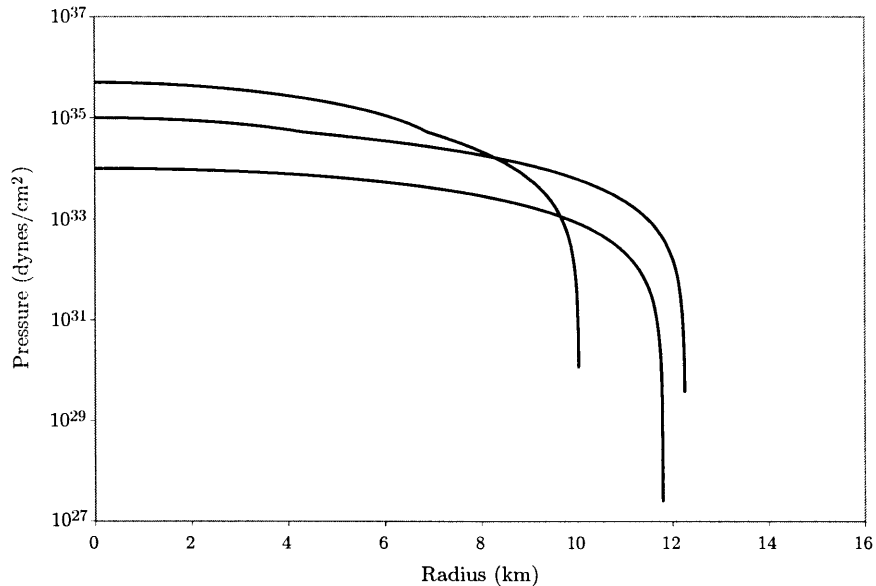


Figure 2-5: Pressure profiles for the static relativistic hybrid neutron star model with central pressures of  $10^{34}$ ,  $10^{35}$ , and  $5 \times 10^{35}$  dynes/cm<sup>2</sup>.

form, even the slightest perturbation to its mass would cause it to collapse into a black hole or to explode outward. Such objects would not exist long enough to be observationally relevant. For the static hybrid neutron star, this sets a limit on the star's maximum central pressure of  $7.14 \times 10^{35}$  dynes/cm<sup>2</sup>, or equivalently, on the star's central gravitational mass density of  $2.86 \times 10^{15}$  g/cm<sup>3</sup>.

Now that we are focused on the relativistic model, we should take a look at typical pressure and density profiles for the hybrid stars based on this model. Fig. 2-5 shows pressure profiles for stars with central pressures of  $10^{34}$ ,  $10^{35}$ , and  $5 \times 10^{35}$  dynes/cm<sup>2</sup>. These central pressures give a stellar model just below the CFL transition, just above the CFL transition, and just below the maximum allowed central pressure established in the last paragraph. As we can see, the pressure remains fairly constant throughout a large part of the volume of the star, and falls to zero very rapidly over only a few hundred meters near its surface. This figure validates the assumptions that went into the zero magnetic field approximation of § 1.3, namely, that the typical mechanical pressures of the relevant neutron star models are at least  $10^{32}$  dynes/cm<sup>2</sup>. A glance

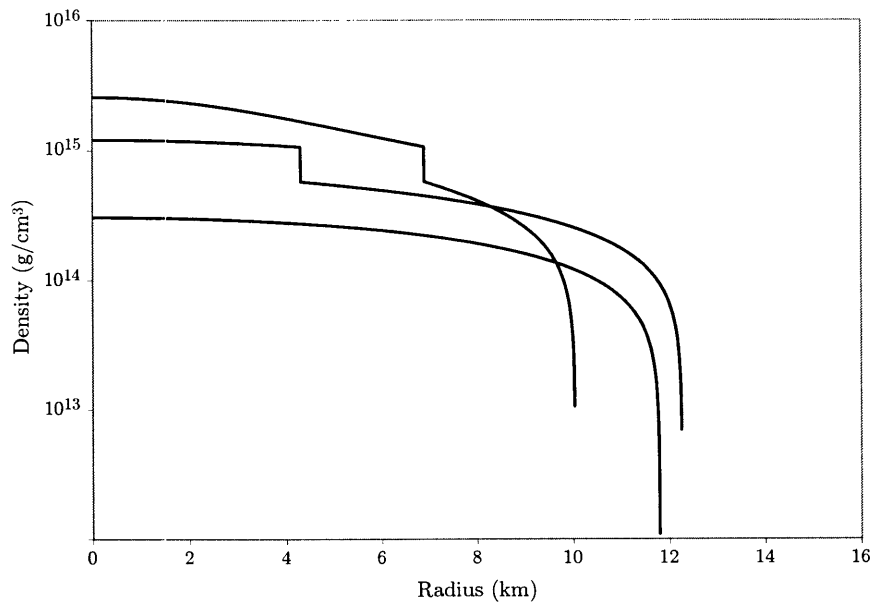


Figure 2-6: Mass-energy density profiles for the static relativistic hybrid neutron star model with central pressures of  $10^{34}$ ,  $10^{35}$ , and  $5 \times 10^{35}$  dynes/cm<sup>2</sup>.

at Fig. 2-5 shows this to be true.

Fig. 2-6 shows mass-energy density profiles for the same stellar models as those in Fig. 2-5. This plot has a few interesting features. First, we note that the curve for the star without CFL matter has no discontinuity in the density whereas the other two do. This is the expected behavior, because the equation of state guarantees that there will be a range of densities at which no part of the star may exist. Additionally, we note that the model just below the CFL transition has a roughly uniform density over much of its interior while the model with the highest central density is not very uniform at all. It has much more of its mass concentrated in its center, which helps to justify the “no crust” approximation of § 1.3.

# Chapter 3

## Rotating Relativistic Models

The next step in this investigation is to look at how hybrid neutron stars behave under slow rotation. As the last chapter indicated, it is not particularly useful to model these stars using Newtonian equations because the errors produced are too large to tolerate. Therefore, we will jump straight into a relativistic treatment of rotating hybrid neutron stars\*.

From a physical point of view, building a relativistic model for a rotating hybrid neutron star is the same as building a relativistic model for a static star; we simply set the star's stress-energy tensor equal to its Einstein curvature tensor and solve the resulting equations. Mathematically, building a relativistic model is far more complicated because the equations are more difficult to solve. While the same relativistic equations of stellar structure and equation of state apply, there are additional complications brought about because rotational energy gravitates and because centrifugal acceleration is not trivial to generalize. Additionally, the body that we are studying is no longer spherically symmetric.

Our analysis of the effect of rotation on a neutron star will begin by examining the effect of the rotation upon the spacetime in and around the star. Understandably, the spacetime around a rotating neutron star is a bit complicated, so we will start by looking at the spacetime around our familiar static, spherically-symmetric star.

---

\*Much of the material in this chapter was derived from Ref. [12]. Rather than citing this source repeatedly, this footnote will serve as a full citation for this chapter. Anything in this chapter whose source is not Ref. [12] will be cited as usual.

### 3.1 The Spacetime of a Static Star

In general relativity, spacetime is described by a metric, a mathematical expression that encodes the distances between any two spacetime events. Outside a spherically-symmetric massive star, the metric is given by the Schwarzschild solution to the Einstein equation

$$ds^2 = - \left(1 - \frac{2M}{r}\right) dt^2 + \frac{dr^2}{1 - 2M/r} + r^2 (d\theta^2 + \sin^2 \theta d\phi^2), \quad (3.1)$$

where  $M$  is the mass of the star [4].

Inside such a star, the metric is not quite the same. It is modified by the fact that the deeper you go into the star, the less mass there is interior to your position, and therefore the less gravity you feel. In Newtonian mechanics, this phenomenon gives rise to Gauss' Law, which allows one to calculate the gravitational potential inside a star of uniform density. In relativity, one can also define a function  $\Phi$  that is the generalization of the Newtonian potential<sup>†</sup>:

$$\frac{d\Phi}{dr} = - \frac{dP/dr}{\rho + P}. \quad (3.2)$$

Given this function, we can write the metric inside a spherically symmetric star as

$$ds^2 = -e^{2\Phi} dt^2 + \frac{dr^2}{1 - 2M/r} + r^2 (d\theta^2 + \sin^2 \theta d\phi^2). \quad (3.3)$$

Of course, because  $\Phi$  is a potential, we are free to set its zero wherever is convenient. Since we know that the interior and exterior solutions must match at the star's surface, we have

$$e^{2\Phi} = 1 - \frac{2M}{r}, \quad (3.4)$$

at the surface<sup>‡</sup>.

---

<sup>†</sup>Note that if we take the Newtonian limit, that is, set  $dP/dr = -GM\rho/r^2$  and  $\rho+P \approx \rho$ , then we recover the Newtonian potential,  $\Phi = -GM/r$

<sup>‡</sup>Note that in the Newtonian limit, that is,  $2M/r \ll 1$ , we again recover the Newtonian potential. Upon restoring  $G$ , we see that  $\Phi = \ln(1-2GM/r)/2 \approx (-2GM/r)/2 = -GM/r$



## 3.2 The Spacetime of a Rotating Star

As is true for most solutions to Einstein's equations, the exact generalization of the static Schwarzschild metric to that of a rotating body typically cannot be written down analytically, with a few interesting exceptions like the Kerr metric for a rotating black hole. However, it is possible to write down an approximate solution if the rotating body is rotating *sufficiently slowly*, because we can treat the effects of rotation as a perturbation to the spherically symmetric model.

There is a subtlety in deciding exactly which rotation we are interested in. As indicated in §1.3, we are making the idealization that our neutron star has a uniform rotation frequency  $\Omega$  as seen by distant observers. However, this is not the rotation rate as seen by a local observer near the star. As the star rotates, it tends to drag spacetime along with it, so that local inertial frames near the surface of the star have a different rotation frequency  $\omega$ , which is a function of  $r$ .

Of course, the fluid making up the star is not in a locally inertial frame, so it experiences centrifugal forces as it rotates. The magnitude of this force is determined by the rate of rotation of the fluid relative to the rate of rotation of the locally inertial frames,  $\tilde{\omega}$ , which equals  $\Omega$  minus  $\omega$ . Thus, in determining the star's structure,  $\tilde{\omega}$  is the frequency we are most interested in.

We will now turn to deciding what “sufficiently slowly” means. One way to think of this is that we want the forces in the star due to rotation to be much smaller than the forces due to gravitation; this will satisfy the requirement that rotation should be a small perturbation added to gravity. Using Newtonian physics, we can estimate the accelerations in the star due to gravity and rotation as

$$a_{grav} = \frac{GM}{r^2} \tag{3.5}$$

$$a_{rot} = \tilde{\omega}^2 r. \tag{3.6}$$

We can then apply the condition that  $a_{rot}$  be much less than  $a_{grav}$  to define an

expansion parameter  $\epsilon$  as

$$\epsilon = \frac{\tilde{\omega}^2 r^3}{GM} \ll 1. \quad (3.7)$$

The condition that the rotation be slow is therefore equivalent to the condition that  $\epsilon$  be small compared to 1.

You may be worried that we used a Newtonian analysis to derive the form of the expansion parameter rather than a relativistic one. This is in fact OK. Relativistic effects tend to make the Newtonian estimate of the gravitational acceleration a bit smaller than it should be, because relativity would add a pressure term to the numerator of  $a_{grav}$  and subtract a mass term from its denominator. Similarly, relativistic effects tend to make the Newtonian estimate of the rotational acceleration a bit bigger than it should be, because the coordinate radius around a massive body is smaller than its proper radius [4]. Both of these effects re-enforce the inequality in Eq. (3.7), making  $\epsilon$  smaller, and therefore more useful as an expansion parameter.

Now that we have a small expansion parameter, we need to decide what is being expanded. Because we are perturbing a spherically symmetric object, the natural thing to do is to expand the metric for the star in a series of Legendre polynomials<sup>§</sup> of the form

$$1 + f(r)P_0 + g(r)P_1 + h(r)P_2 + \dots, \quad (3.8)$$

where the  $P_n$  are Legendre polynomials.

Given all this, it is now time to introduce the metric for the rotating star:

$$\begin{aligned} ds^2 = & -e^{2\Phi}[1 + 2(h_0 + h_2P_2)]dt^2 + \left[1 + \frac{2(m_0 + m_2P_2)}{r - 2M}\right] \frac{dr^2}{1 - 2M/r} \\ & + r^2[1 + 2(v_2 - h_2)P_2] \left[d\theta^2 + \sin^2\theta(d\phi - \omega dt)^2\right], \end{aligned} \quad (3.9)$$

where  $P_2$  is the Legendre polynomial given by

$$P_2 = \frac{3 \cos^2 \theta - 1}{2}, \quad (3.10)$$

---

<sup>§</sup>Legendre polynomials are complete and orthogonal, which makes them a useful set of functions to use in a series expansion. Furthermore, they are related to the spherical harmonics, which give the angular dependence of certain deformations of spherical objects.

and where  $h_0$ ,  $h_2$ ,  $m_0$ ,  $m_2$ , and  $v_2$  are new functions that depend only on  $r$  and that characterize the amount of deformation of the star due to rotation. As in Newtonian theory, these deformations can be thought of as due to centrifugal flattening and so will scale as  $\tilde{\omega}^2$ . Additionally, we note that the five deformation functions have two different subscripts: 0 and 2. The functions with a subscript of 0 represent rotational deformations to the star that are spherical, that is, that have no angular dependence<sup>¶</sup>. The functions with a subscript of 2 represent rotational deformations to the star that are quadrupolar, that is, that have angular dependence that looks like  $P_2$ .

With this interpretation, it becomes much clearer where the new metric as a whole comes from. Each component of the original metric is multiplied by a factor that looks like Eq. (3.8)<sup>||</sup> because the new metric is a Legendre polynomial expansion of the Schwarzschild metric. While not evident from the metric, the five deformation functions are all proportional to  $\epsilon$ , so terms which are higher order in  $\epsilon$  have been neglected in this approximation. If we stay in a region of parameter space where  $\epsilon$  is small, this is a valid approximation of the metric of a rotating neutron star.

It can be proven [13], although it is beyond the scope of this thesis to do so, that the new metric provides sufficient functional freedom to specify a rotating star. Intuitively, one can see that enough functions have been provided to allow the diagonal components of the metric to vary in both a spherical and quadrupolar manner from their static equivalents; the off-diagonal component of the metric is added to account for frame dragging. These functions are fixed by requiring that this metric satisfy the Einstein field equations for a rotating, axisymmetric fluid body to order  $\tilde{\omega}^2$ .

In addition to the five deformation functions in the metric, there are two additional functions that are necessary to describe the change in the pressure of the star due to rotation:  $p_0$  and  $p_2$ . They are defined by

$$P_{total} = P + (P + \rho)(p_0 + p_2 P_2), \quad (3.11)$$

---

<sup>¶</sup>If you like, you can think of these quantities as being multiplied by  $P_0$ , the Legendre polynomial that is identically 1 and therefore has no angular dependence.

<sup>||</sup>Because of symmetry, there is no term proportional to  $P_1 = \cos \theta$ , which represents a shift of the center of mass.

where the  $P$  and  $\rho$  on the right hand side are the pressure and density of the static star with the same central pressure\*\*. Together  $h_0, h_2, m_0, m_2, v_2, p_0, p_2,$  and  $\omega$  completely describe the effects of rotation to the neutron star given the assumption of slow rotation.

As is stated above, these functions are fixed by application of the Einstein field equations to the metric. This rather laborious calculation is done in [13]. After the mathematical dust settles, we find that these functions are determined by relatively simple ordinary differential equations. We now turn to a presentation and discussion of these ODEs.

### 3.2.1 Spin Frequency and Angular Momentum

The first step in this process is to calculate the rotational frequency of the star  $\tilde{\omega}$ . As it happens,  $\tilde{\omega}$  obeys the second-order differential equation

$$j \frac{d^2 \tilde{\omega}}{dr^2} + \frac{4j}{r} \frac{d\tilde{\omega}}{dr} + \frac{dj}{dr} \frac{d\tilde{\omega}}{dr} + \frac{4\tilde{\omega}}{r} \frac{dj}{dr} = 0, \quad (3.12)$$

where  $j$  is a function given by

$$j = e^{-\Phi} \left( 1 - \frac{2M}{r} \right)^{1/2}, \quad (3.13)$$

that depends only on the spherical metric. Given this set of equations and some boundary conditions, we can solve for  $\tilde{\omega}$ . At the center of the star,  $d\tilde{\omega}/dr=0$  and  $\tilde{\omega}$  equals some nonzero value that is determined by the value of  $\Omega$ , as we will see below.

Given  $\tilde{\omega}$ , we can determine the star's spin angular momentum  $S$  as

$$S = \frac{1}{6} R^4 \left. \frac{d\tilde{\omega}}{dr} \right|_{r=R}, \quad (3.14)$$

---

\*\*In general, quantities like  $P, M, \rho,$  and so on refer to those quantities for the static star.

where  $r=R$  is the surface of the star<sup>††</sup>. Because we must have

$$\tilde{\omega}(r) = \Omega - \frac{2S}{r^3}, \quad (3.15)$$

in the star's exterior, we know that at the star's surface we have

$$\Omega = \tilde{\omega}(R) + \frac{2S}{R^3}. \quad (3.16)$$

This matching condition sets the value of  $\tilde{\omega}$  at the star's center based on the value of  $\Omega$ , as promised.

Finally, we can calculate one more interesting quantity, the star's moment of inertia  $I$ , by defining

$$I \equiv \frac{S}{\Omega}. \quad (3.17)$$

This is a very convenient and simple formula. It is certainly correct for a far-away observer, who sees the system as Newtonian, but since all observers should agree on the value of  $I$  for the star, it must give the correct  $I$  in general.

As a final note before moving on to the rotating metric, you may be worried that the condition  $r=R$  used above seems to imply a spherical star, whereas a rotating star should be oblate. This is not actually a problem because  $r$  is the *coordinate radius* for the metric, not the *proper radius* of the star. The proper radius of the star is the radius an observer looking at the star would see; for a rotating star, the proper radius at its equator is greater than the proper radius at its poles. On the other hand, the coordinate radius is just a convenient way to represent the radial coordinate in the metric. The coordinate radius and proper radius are of course related mathematically, but the exact form of that relationship is a choice made by writing the metric in a particular way. We have made the useful choice that the coordinate radius at the surface of the star has the same value all over the surface in order to make the calculations easier.

---

<sup>††</sup>Note that the statement that  $r=R$  is a subtle one for an oblate object; we will return to this point shortly.

### 3.2.2 Spherical Deformations

The spherical mass and pressure deformations are given by a pair of coupled differential equations:

$$\frac{dm_0}{dr} = 4\pi r^2 \frac{d\rho}{dP} (\rho + P) p_0 + \frac{1}{12} j^2 r^4 \left( \frac{d\tilde{\omega}}{dr} \right)^2 - \frac{2}{3} r^3 \tilde{\omega}^2 j \frac{dj}{dr}, \quad (3.18)$$

and

$$\begin{aligned} \frac{dp_0}{dr} &= -\frac{1 + 8\pi r^2 P}{(r - 2M)^2} m_0 - \frac{4\pi r^2 (\rho + P)}{r - 2M} p_0 \\ &+ \frac{1}{12} \frac{r^4 j^2}{r - 2M} \left( \frac{d\tilde{\omega}}{dr} \right)^2 + \frac{1}{3} \frac{d}{dr} \left[ \frac{r^3 j^2 \tilde{\omega}^2}{r - 2M} \right], \end{aligned} \quad (3.19)$$

subject to the condition that both  $m_0$  and  $p_0$  vanish at the center of the star.

Once we know  $m_0$ , we can calculate the total mass of the star to be

$$M_{total} = M(R) + m_0(R) + \frac{S^2}{R^3}. \quad (3.20)$$

This mass, called the *gravitational mass*, includes both the rest mass of the star, the negative contribution to the mass due to the gravitational binding energy of the star, and the positive contribution due to rotational kinetic energy. We will discuss how to calculate the rest mass of the star alone in § 3.4.

### 3.2.3 Quadrupolar Deformations

The quadrupolar deformations are also given by a set of coupled differential equations:

$$\frac{dv_2}{dr} = -2h_2 \frac{d\Phi}{dr} + \left( \frac{1}{r} + \frac{d\Phi}{dr} \right) \left[ \frac{1}{6} j^2 r^4 \left( \frac{d\tilde{\omega}}{dr} \right)^2 - \frac{2}{3} r^3 \tilde{\omega}^2 j \frac{dj}{dr} \right] \quad (3.21)$$

and

$$\frac{dh_2}{dr} = \left\{ -2 \frac{d\Phi}{dr} + \frac{r}{2(r - 2M)} \left( \frac{d\Phi}{dr} \right)^{-1} \left[ 8\pi(\rho + P) - \frac{4M}{r^3} \right] \right\} h_2$$

$$\begin{aligned}
& - \frac{2v_2}{r(r-2M)} \left( \frac{d\Phi}{dr} \right)^{-1} + \frac{1}{6} \left[ r \frac{d\Phi}{dr} - \frac{1}{2(r-2M)} \left( \frac{d\Phi}{dr} \right)^{-1} \right] r^3 j^2 \left( \frac{d\tilde{\omega}}{dr} \right)^2 \\
& - \frac{2}{3} \left[ r \frac{d\Phi}{dr} + \frac{1}{2(r-2M)} \left( \frac{d\Phi}{dr} \right)^{-1} \right] r^2 \tilde{\omega}^2 j \frac{dj}{dr}, \tag{3.22}
\end{aligned}$$

subject to the condition that  $h_2$  and  $v_2$  vanish at the center of the star.

Since we are discussing quadrupolar deformations, this is an appropriate time to talk about the eccentricity of the hybrid neutron stars. Because they are made of two distinct types of matter, the hybrid neutron stars should have an eccentricity that varies between the star's center and its surface. In order to calculate the eccentricity, we need to know  $p_2$ . Fortunately, this function is a simple combination of ones we already know:

$$p_2 = -h_2 - \frac{1}{3} r^2 e^{-2\Phi} \tilde{\omega}^2 \tag{3.23}$$

Given this, we can express the proper radius of the star as

$$r_{proper} = r + \xi_0 + \xi_2 P_2, \tag{3.24}$$

where

$$\xi_0 = -p_0 \left( \frac{d\Phi}{dr} \right)^{-1}, \tag{3.25}$$

and

$$\xi_2 = -p_0 \left( \frac{d\Phi}{dr} \right)^{-1}. \tag{3.26}$$

We can then find the mean radius of the star to be

$$\bar{r}_{proper} = r + \xi_0, \tag{3.27}$$

while the eccentricity is

$$e(r) = \left[ 3 \left( h_2 - v_2 - \frac{\xi_2}{r} \right) \right]^{1/2}. \tag{3.28}$$

This eccentricity is due to centrifugal flattening of the star.

### 3.3 The Baryon Mass

In order to compare the effects of rotation on the same star rotating at different rates, we need a criterion for deciding when two stellar models with different central pressures and angular velocities represent the same star. If we imagine a neutron star stationary in space and then imagine spinning it up, the only characteristic of the star that remains constant is the rest mass, or *baryon mass*, of the star. Therefore, we need to be able to calculate the baryon mass to ensure that we are not comparing apples with oranges when we compare two stellar models.

For a spherical neutron star, the baryon mass is given by

$$\begin{aligned} M_{B,spherical} &= \int_0^R \rho_0 dV_{proper} \\ &= \int_0^R 4\pi r^2 \rho_0 \left(1 - \frac{2M}{r}\right)^{-1/2} dr. \end{aligned} \quad (3.29)$$

As was the case with the other quantities we looked at, the baryon mass is modified by the rotation of the star. For a rotating star, we find that

$$M_B = M_{B,spherical} + m_0(R) + \int_0^R 4\pi r^2 B(r) dr, \quad (3.30)$$

where  $B(r)$  is given by

$$\begin{aligned} B(r) &= (\rho + P)p_0 \left[ \frac{d\rho_0}{dP} \left(1 - \frac{2M}{r}\right)^{-1/2} - \frac{d\rho}{dP} \right] + \frac{1}{6\pi} j \frac{dj}{dr} r \tilde{\omega}^2 \\ &+ \rho_0 \left(1 - \frac{2M}{r}\right)^{-3/2} \left[ \frac{m_0}{r} + \frac{1}{3} j^2 r^2 \tilde{\omega}^2 \right] - \frac{1}{48\pi} j^2 r^2 \left( \frac{d\tilde{\omega}}{dr} \right)^2. \end{aligned} \quad (3.31)$$

With these relationships, we can calculate the baryon mass of any rotating neutron star.



# Chapter 4

## Rotating Relativistic Results

Now that we have gone through the theory for the rotating relativistic neutron star models, it is time to look at some numerical results. Since our stars are now rotating, there are two parameters, the central pressure and the angular velocity, governing the behavior of the stellar models. This results in a much larger parameter space of models available for investigation. Our first order of business will be to restrict the parameter space of interest by finding upper limits on the central pressure and angular velocity of the stars. We can then look into other interesting properties of these models that come with rotation.

### 4.1 Verifying the Slow Spin Approximation

In the last chapter, we argued that in order for Eq. (3.9) to be the correct metric for a rotating neutron star, the star needs to rotate sufficiently slowly. We characterized the slowness of the rotation by introducing the expansion parameter  $\epsilon$ , and we claimed that  $\epsilon$  had to be much smaller than unity in order for our approximation to be valid.

In order to determine the conditions under which  $\epsilon$  is small, we plot  $\epsilon$  as a function of coordinate radius for several stellar models in Fig. 4-1. Each of the models shown has a central density of  $2 \times 10^{34}$  dynes/cm<sup>2</sup>, which was chosen because it is in the range of pressures between the transition pressure and upper pressure limit for stability of static neutron stars determined in § 2.5. Each curve in this plot represents

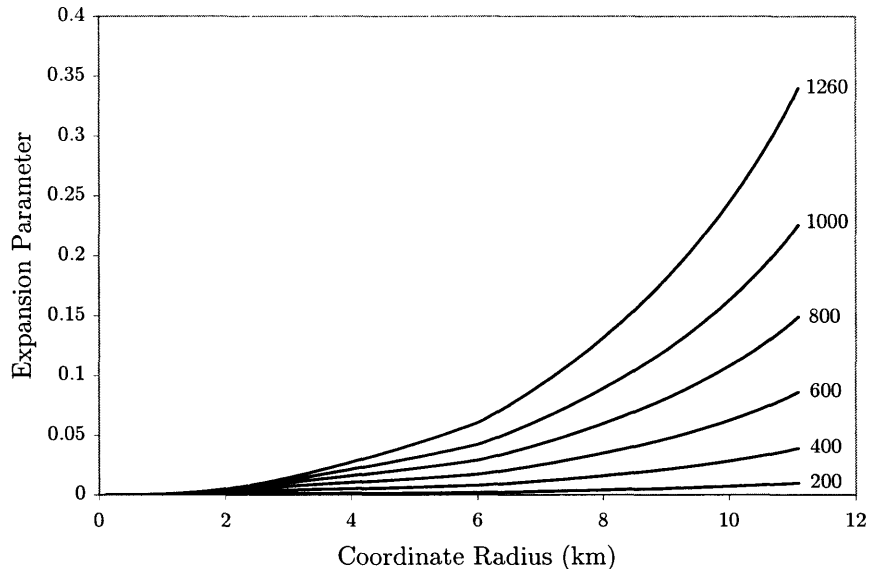


Figure 4-1: The value of the slow spin parameter as a function of coordinate radius for various rotating neutron star models. All of these models have a central pressure of  $2 \times 10^{35}$  dynes/cm<sup>2</sup>. The labels next to each curve gives the angular velocity  $\Omega$  of each model in rad/s.

a different angular velocity  $\Omega$  for the star, ranging from 200 rad/s to 1260 rad/s\*.

Based on this plot, we can make some reasonable statements about how accurate our slow spin approximation really is. First of all, it is true for all of our stellar models that the approximation is better towards the center of the star than near its surface. This makes sense because we expect the  $\tilde{\omega}^2 r^3$  in the numerator of the expansion parameter to dominate over the  $m$  in the denominator. This is convenient for our specific models because they are very centrally condensed. In general, we care much more that the slow spin approximation be good where most of the mass of the star is, that is, in the central CFL region.

On the other hand, what we really want is for the slow spin approximation to hold across the entire star, which means that we'd like  $\epsilon$  to be smaller than some cutoff value for all  $r$ . The choice of this cutoff value is a bit arbitrary and depends on how much error we are willing to accept in our results. If we decide that an error of about 10 percent in the outermost layer is acceptable, that is, if  $\epsilon \approx 0.1$ , then Fig. 4-1

---

\*For those more used to frequencies in Hertz, that's 32 and 200 Hz, respectively.

gives the maximum angular velocity for which we trust our results to be about 600 rad/s. Certainly we should not trust any results for stars rotating faster than about 700 rad/s. If we restrict  $\epsilon$  to be less than 0.05, then we get the more conservative maximum angular velocity of about 400 rad/s, below which the approximation is certainly good.

One interesting question to ask is how these cutoff velocities compare to neutron stars found in nature. The Princeton Pulsar Catalog [14] lists 706 pulsars. Of these, only 53 have frequencies greater than 250 rad/s. Although this catalog is a bit out of date, the fraction of slowly rotation neutron stars has remained about the same as pulsar surveys have expanded [15]. In other words, between 90 and 95 percent of all known pulsars easily fall into the slow spin approximation.

One interesting extension of this work on hybrid neutron stars would be to study their behavior in binary systems. One very well-known relativistic binary system is 1913+16<sup>†</sup>; the pulsar in this system has a rotation rate of 106 rad/s [14]. Similarly, the pulsars in the recently-discovered binary J0737-3039 have rotation rates of 277 and 2.27 rad/s [16]. This suggests that the slow spin approximation should be good for the neutron stars found in binaries so far.

## 4.2 Spin and Baryon Mass

In § 2.5, we argue that there is a maximum stable mass for the static neutron stars. This is still true when the stars are rotating; the rate of rotation simply changes the maximum mass. Because the star is rotating, it has both mechanical and centrifugal forces to counteract the gravitational forces acting to collapse the star. This means that the faster the star spins, the greater its centrifugal forces and the more mass it can support.

Fig. 4-2 is a plot of baryon mass versus central pressure for stellar models with different angular velocities. The maximum of each curve indicates the maximum mass

---

<sup>†</sup>This is the binary system whose discovery won Joseph Taylor and Russel Hulse the Nobel Prize in 1993.

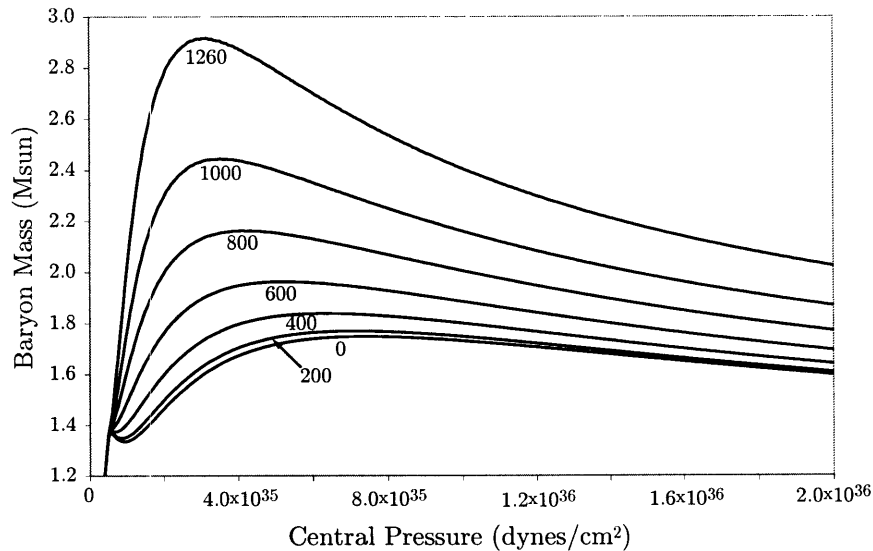


Figure 4-2: Baryon mass as a function of central pressure for a variety of different angular velocities. The angular velocity labels are in rad/s.

sustainable by a neutron star at that curve's particular angular velocity. As expected, the maximum mass increases with increasing  $\Omega$ . We can make the same argument as we did for the static mass-pressure plot to show that the parts of the curves to the right of the maximum are unstable.

In addition to increasing the maximum mass, faster rotation also decreases the maximum central density of a rotating neutron star. This phenomenon is illustrated by Fig. 4-3, which shows curves of constant baryon mass plotted in the central pressure-angular velocity plane. Curves of constant baryon mass can be thought of as a star of a particular mass evolving through a series of states as its rotation rate changes. We can see from the plot that there are two classes of constant-mass curves: those that touch the central pressure axis and those that curve up away from it. The former are curves for stars whose baryon masses are below the maximum mass allowed for static stars, and the latter are curves for stars whose masses are so large that they cannot exist at zero angular velocity.

A little thought experiment can help to illustrate the relationship between angular velocity and central pressure for the first type of curve. Imagine a static star of

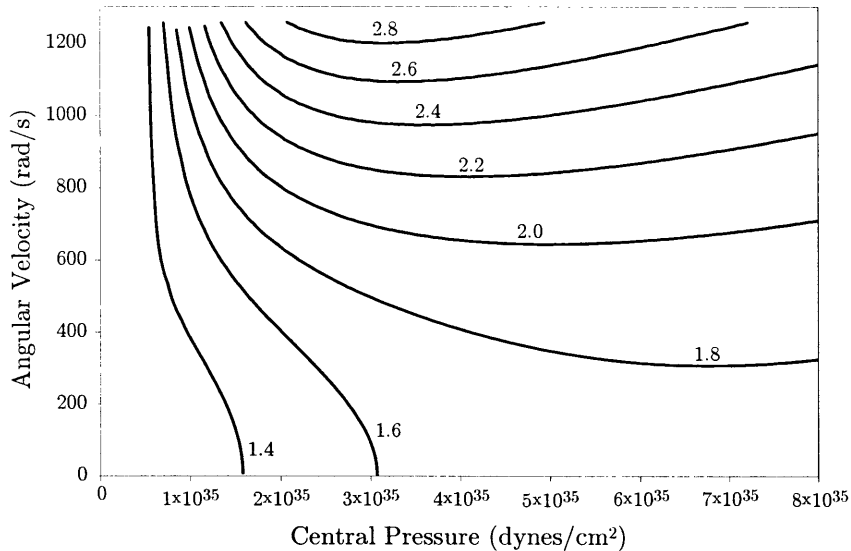


Figure 4-3: Curves of constant baryon mass plotted in the central pressure-angular velocity plane. The masses labelling each curve are in solar masses.

particular baryon mass and central pressure in space, and then imagine that it starts to spin. As the star spins up, its baryon mass stays the same, but its central pressure decreases because centrifugal forces push the matter in the star outwards. Therefore, we expect there to be an inverse relationship between  $P_{central}$  and  $\Omega$ , which we see in this plot for all of the curves that exist at  $\Omega=0$ .

The second type of curve requires a bit more explaining. These curves represent stars that cannot exist at zero angular velocity because they would be unstable under that condition; instead, they each have a minimum nonzero angular velocity for which they are stable. Given this condition, the section of each curve to the left of its minimum behaves exactly as described in the thought experiment of the preceding paragraph. On the other hand, the curve to the right of each minimum behaves in the opposite fashion, indicating that these are unstable configurations for these neutron star models that cannot exist.

The fact that these stars cannot exist at  $\Omega=0$  in no way makes them unphysical. Neutron stars form from the death of actively burning stars, which themselves form from swirling clouds of dust. All along the way, angular momentum must be con-

served, so neutron stars are born with a nonzero  $\Omega$  as a rule. This means that, in principle, they can be born in any region of  $\Omega$ - $P_{central}$  pressure parameter space where these two quantities have an inverse relationship. We should, however, take Fig. 4-3 with a grain of salt; since we know that the slow spin approximation is not very good above about 600 rad/s, we cannot really trust the results in that figure above that value of angular velocity.

### 4.3 Eccentricity and Angular Momentum

When a star rotates, we expect that it will be oblate rather than round because centrifugal forces will cause the matter around the star’s equator to expand outwards. This is true for our hybrid neutron stars as well. Because these hybrid stars have two distinct regions governed by different parts of the hybrid equation of state, we expect that eccentricity will not be uniform across the star. In particular, we expect that the outer regions will have a higher eccentricity because the matter there is less tightly bound.

Fig. 4-4 shows a plot of eccentricity as a function of coordinate radius for various angular velocities. We see immediately the expected behavior that the eccentricity increases with radius. We also notice that for higher rotation rates the eccentricities become anomalously large, to the point of exceeding 1 for the highest angular velocities. This is more confirmation that the slow spin approximation breaks down for angular velocities that are this high.

The final interesting result we produced from the rotating star model has to do with an instability called the *backbending instability*. Originally discovered in the study of heavy nuclei, this phenomenon has been computationally “observed” for neutron stars, which can be thought of as huge nuclei, in [17]. The backbending instability is related to the moment of inertia of the star. We know from basic mechanics that the relationship between the angular velocity and angular momentum  $S$  of a body is

$$S = I\Omega, \tag{4.1}$$

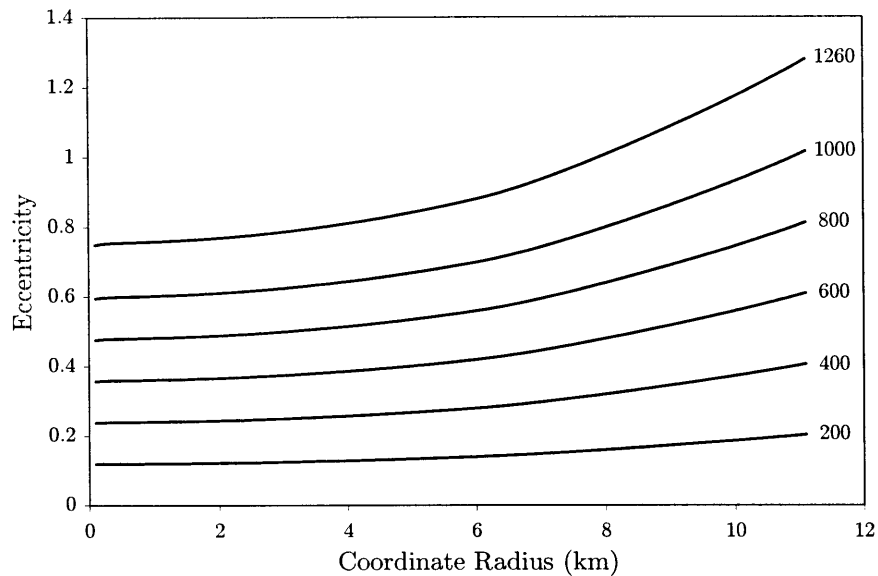


Figure 4-4: The eccentricity of various rotating neutron star models as a function of coordinate radius for a variety of angular velocities. All of these models have a central pressure of  $2 \times 10^{35}$  dynes/cm<sup>2</sup>. The angular velocity labels are in units of rad/s.

where  $I$  is the moment of inertia. The backbending instability is characterized by a negative moment of inertia, which is clearly not allowed.

Fig. 4-5 shows a plot of spin versus angular velocity for a number of different baryon masses. Given Eq. (4.1), the slope of a curve at a point along it is the moment of inertia for that particular stellar model. We see that most areas of the curves are positively sloped, which is what we expect. However, all curves other than the one with the lowest mass include a region where the curve turns around in such a way that the moment of inertia goes negative in a small region of parameter space. This is the backbending instability. Regions of the curves right around the turnaround points are forbidden.

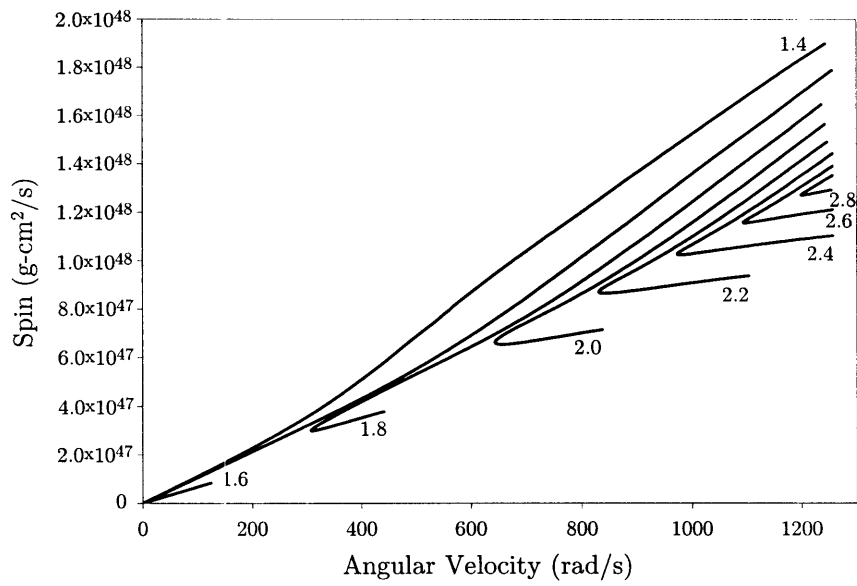


Figure 4-5: Curves of constant baryon mass plotted in the angular velocity-spin plane. The baryon mass labels are in units of solar masses.



# Chapter 5

## Conclusions

We conclude by reviewing what we have achieved and by posing some natural directions to push this work further.

### 5.1 Where have we been?

First, we were able to build stellar models, both for rotating and static neutron stars, with the hybrid equation of state. This is not something that had been done with rotating models before, so it was not clear that it would work all that well. We were able to do it for both Newtonian and relativistic models. We were also able to extend the Lane-Emden formalism, described in Appendix B, to the hybrid equation of state. This is an important first step, because without knowing how to incorporate the hybrid equation of state into physical models, there would be no way to study it.

In addition to creating the models, we were able to determine bounds on the physical conditions to which they applied. We placed reasonable bounds on how strong the magnetic field of a neutron star could be in order for our approximations to apply. We also set bounds on the maximum rotation rate supported by our models, and noted that the large majority of known neutron stars have rotation rates lower than this cutoff.

Finally, we verified that the backbending instability for neutron stars discussed in [17] also applies to the hybrid equation of state. We also found this instability using

far less computational horsepower than the authors of [17] used. The computational simplicity of our modelling methods was helpful in generating quick but accurate results.

## 5.2 Where do we go from here?

This thesis has laid the groundwork for studies of realistic neutron star models based on the CFL hybrid equation of state. An important property of these models is that their masses and radii are not substantially different from the masses and radii of typical neutron star models. Indeed, this is why this equation of state has not been ruled out already; its predictions are consistent with current observations of neutron stars given observational error. This suggests that future tests of the CFL model will be based on their *dynamical* behavior.

An important example of such future work would be a study of the disruption characteristics of hybrid neutron stars. Neutron stars in a compact binary system with another neutron star or a black hole will spiral towards one another as they lose energy by gravitational wave emission. Eventually, the members of the binary will come close enough that their tidal effects on one another will distort their structure, eventually tearing the neutron star apart. Because it is made of two different phases of matter, a hybrid neutron star is likely to exhibit rather different disruption behavior than a typical, one-phase neutron star. These differences may be manifest in the gamma-ray or gravitational radiation produced during the disruption.

Since we have shown that Newtonian models are completely inadequate to model hybrid CFL neutron stars, an approach based on the Newtonian theory of tidal interactions is out of the question\*. However, it should be possible to incorporate *relativistic* tidal effects into our model of these stars by using perturbation theory in a manner similar to that of the slow spin approximation. Roughly speaking, we should be able to generalize the metric in a manner consistent with the flattening

---

\*In fact, our original goal was to avoid the complications of relativity and perform an analysis of tidal disruption using Newtonian theory, as in [18]. Clearly, this did not work.

effects we expect for a body in a tidal field and then fix free functions in this metric by applying the Einstein field equations. Such an analysis is far beyond the scope of what we have done here, and would require much additional labor and analysis. We leave this for some future thesis advisee to handle.



# Appendix A

## On Units

Several different unit systems were involved in the making of this thesis, each one useful for a different aspect of it. Because of this, doing everything in one unit system was not feasible, so keeping track of conversion factors was quite important.

There were three important dimensionful quantities given as inputs into the equation of state: the transition pressure  $P_T$  and the two transition densities  $\rho_{CFL}$  and  $\rho_{nuc}$ . These quantities were originally expressed in the literature in nuclear physics units, where pressures and densities are both measured in units of  $\text{MeV}/\text{fm}^3$ ; we had  $P_T = 32.67 \text{ MeV}/\text{fm}^3$ ,  $\rho_{CFL} = 595.5 \text{ MeV}/\text{fm}^3$ , and  $\rho_{nuc} = 313.9 \text{ MeV}/\text{fm}^3$ . To convert to cgs, we use the factors

$$1 \frac{\text{MeV}}{\text{fm}^3} = 1.6022 \times 10^{33} \frac{\text{dynes}}{\text{cm}^2}, \quad (\text{A.1})$$

$$1 \frac{\text{MeV}}{\text{fm}^3} \frac{1}{c^2} = 1.7827 \times 10^{12} \frac{\text{g}}{\text{cm}^3}. \quad (\text{A.2})$$

This gives  $P_T = 5.234 \times 10^{34} \text{ g}/\text{cm}\cdot\text{s}^2$ ,  $\rho_{CFL} = 1.062 \times 10^{15} \text{ g}/\text{cm}^3$ , and  $\rho_{nuc} = 5.596 \times 10^{14} \text{ g}/\text{cm}^3$ .

For the relativistic calculation, we followed the usual convention of relativity by setting  $G=c=1$ . We chose to express all of the resulting quantities in terms of the km. Some useful quantities that result from this choice are

$$1\text{s} = 3.00 \times 10^5 \frac{1}{c} \text{ km} \quad (\text{A.3})$$

$$1\text{g} = 7.425 \times 10^{-34} \frac{c^2}{G} \text{ km} \quad (\text{A.4})$$

$$1 \frac{\text{g}}{\text{cm} \cdot \text{s}^2} = 8.216 \times 10^{-40} \frac{c^4}{G} \text{ km}^{-2} \quad (\text{A.5})$$

$$1 \frac{\text{g}}{\text{cm}^3} = 7.425 \times 10^{-19} \frac{c^2}{G} \text{ km}^{-2}. \quad (\text{A.6})$$

We note that both pressure and density are measured in  $\text{km}^{-2}$  and that length, time, and mass are all measured in km. In these units, the quantities of interest in the equation of state are  $P_T = 4.324 \times 10^{-5} \text{ km}^{-2}$ ,  $\rho_{CFL} = 7.885 \times 10^{-4} \text{ km}^{-2}$ , and  $\rho_{nuc} = 4.155 \times 10^{-4} \text{ km}^{-2}$ .

# Appendix B

## The Lane-Emden Solution

To solve the equations of stellar structure with a given equation of state, it is often useful to put them into a dimension-free form. The result is known as the Lane-Emden equation. By solving the Lane-Emden equation once, it is possible to find a family of solutions to the equations of stellar structure related to each other by simple scaling relations. While we ultimately did not use this method to calculate stellar models for this study, it is quite standard to use it when studying stellar models with a polytropic equation of state.

Before deciding to solve our stellar models without using the Lane-Emden method, we developed a way to apply the Lane-Emden formalism to the hybrid equation of state. Because this solution was surprisingly elegant, we will include it here\*.

### B.1 The Method

The equations of stellar structure can be combined into the second order ODE

$$\frac{1}{r^2} \frac{d}{dr} \left( \frac{r^2}{\rho} \frac{dP}{dr} \right) = -4\pi G \rho, \quad (\text{B.1})$$

---

\*The solution to the Lane-Emden equation for a polytrope presented here was follows the treatment of the topic in [5].

by solving for mass in Eq. (2.2) and plugging the result into Eq. (2.1). One can then make a change of variables for  $r$

$$r \equiv a\xi, \quad (\text{B.2})$$

where  $a$  carries the dimensions of length and  $\xi$  is a new, dimensionless variable. The analytic form of  $a$  depends on the equation of state chosen. Substituting this into Eq. (B.1) produces

$$\frac{1}{\xi^2} \frac{d}{d\xi} \left( \frac{\xi^2}{\rho} \frac{dP}{d\xi} \right) = -4\pi G \rho a^2. \quad (\text{B.3})$$

This is as far as we can get without specifying an equation of state.

### B.1.1 Polytropic

We will begin by going through the Lane-Emden derivation for the polytropic equation of state to show how it is typically done. We will proceed by inverting Eq. (2.7),

$$\rho = \left( \frac{P}{k} \right)^{n/n+1} \quad (\text{B.4})$$

$$= \left( \frac{P}{k} \right)^{1/\Gamma}, \quad (\text{B.5})$$

where we have defined  $\Gamma = 1 + 1/n$  for calculational convenience. We can use this result to eliminate  $\rho$  from Eq. (B.1):

$$\frac{1}{\xi^2} \frac{d}{d\xi} \left( \xi^2 P^{-n/n+1} \frac{dP}{d\xi} \right) = -\frac{4\pi G}{k^{2n/n+1}} a^2 P^{n/n+1}. \quad (\text{B.6})$$

In order to continue, we define a second dimensionless parameter  $\theta$  such that

$$P \equiv \mathcal{P} \theta^{n+1}, \quad (\text{B.7})$$

where  $\mathcal{P}$  is a constant that carries the dimensions of pressure and  $n$  is the same as the  $n$  in Eq. (2.7). Differentiating this expression with respect to  $\xi$  allows us to evaluate



the derivative of  $P$  that appears in Eq. (B.6) as

$$\frac{dP}{d\xi} = \mathcal{P} (n+1) \theta^n \frac{d\theta}{d\xi}. \quad (\text{B.8})$$

We can now substitute the expressions for  $P$  and  $dP/dr$  into Eq. (B.6), producing

$$\frac{1}{\xi^2} \frac{d}{d\xi} \left( \xi^2 \frac{d\theta}{d\xi} \right) = -\theta^n a^2 \frac{4\pi G}{n+1} \frac{\mathcal{P}^{n-1/n+1}}{k^{2n/n+1}}. \quad (\text{B.9})$$

The right side of this expression looks messy, but it is in fact mostly a bunch of constants. We will define these constants away by cleverly choosing  $a$  such that

$$a^2 \equiv \frac{n+1}{4\pi G} \frac{k^{2n/n+1}}{\mathcal{P}^{n-1/n+1}}. \quad (\text{B.10})$$

The dimensionless L-E equation for a polytrope is therefore

$$\frac{1}{\xi^2} \frac{d}{d\xi} \left( \xi^2 \frac{d\theta}{d\xi} \right) = -\theta^n. \quad (\text{B.11})$$

In order to numerically solve this second-order differential equation, it is convenient to rewrite it as a system of two first-order differential equations. We proceed by expanding out the nested derivatives in Eq. (B.11), producing

$$\frac{d^2\theta}{d\xi^2} + \frac{2}{\xi} \frac{d\theta}{d\xi} + \theta^n = 0. \quad (\text{B.12})$$

We then define a new variable  $q$

$$q \equiv \theta', \quad (\text{B.13})$$

where we use the notation that a prime on a variable represents a derivative with respect to  $\xi$ . This may be substituted into Eq. (B.12), giving

$$q' + \frac{2}{\xi} q + \theta^n = 0. \quad (\text{B.14})$$

Eqs. (B.13) and (B.14) are the system of first-order equations we desired.

All that now remains to solve these equations is to specify boundary conditions. At the center of the star, where  $\xi=0$  (or equivalently, where  $r=0$ ), we need to set the values of  $\theta$  and  $q$ . If we choose  $\mathcal{P}$  to equal the pressure at the center of the star, that is,

$$P(r = 0) = \mathcal{P}, \quad (\text{B.15})$$

then Eq. (B.7) implies that

$$\theta(\xi = 0) = 1. \quad (\text{B.16})$$

The initial condition on  $q$  is a bit harder to derive. From Eq. (B.8), we see that  $q$  is proportional to  $dP/dr$  at  $r=0$  because we can set  $\theta$  equal to 1 by Eq. (B.16). Therefore,

$$q(\xi = 0) = \lim_{\xi \rightarrow 0} q = \lim_{r \rightarrow 0} \frac{dP}{dr}. \quad (\text{B.17})$$

Substituting Eqs. (2.2) and (2.1) and using L'Hôpital's rule, we find

$$\begin{aligned} \lim_{r \rightarrow 0} \frac{dP}{dr} &= \lim_{r \rightarrow 0} \frac{-Gm\rho}{r^2} \\ &= -G \lim_{r \rightarrow 0} \frac{m}{r^2} \cdot \lim_{r \rightarrow 0} \rho \\ &= -G\rho(r = 0) \lim_{r \rightarrow 0} \frac{dm/dr}{2r} \\ &= -G\rho(r = 0) \lim_{r \rightarrow 0} \frac{4\pi\rho r^2}{2r} \\ &= 0, \end{aligned} \quad (\text{B.18})$$

which implies that

$$q(\xi = 0) = 0. \quad (\text{B.19})$$

The other boundary of interest is the boundary between the star and space. Because pressure must always be continuous,  $P=0$  at the surface of the star, which implies that  $\theta=0$  there also. Because of the form of the polytropic equation of state, we know that  $\rho=0$  at that boundary as well. This set of conditions is the signal that integration of the Lane-Emden equation should stop.

## B.1.2 Linear

The method of applying the Lane-Emden formalism to a polytropic equation of state is standard. Because the hybrid neutron star's equation of state has a piece which is linear, we will now extend our treatment of the Lane-Emden technique to apply it to a linear equation of state:

$$\rho = \alpha + \beta P, \quad (\text{B.20})$$

where  $\alpha$  carries the dimension of a mass density and  $\beta$  carries the dimension of inverse velocity squared<sup>†</sup>. Following the method of the previous section, we use the linear equation of state to eliminate  $\rho$  in Eq. (B.3), producing

$$\frac{1}{\lambda^2} \frac{d}{d\lambda} \left( \frac{\lambda^2}{\alpha + \beta P} \frac{dP}{d\lambda} \right) = -4\pi G (\alpha + \beta P) b^2. \quad (\text{B.21})$$

Note that we have changed notation a bit for clarity: the variable  $\xi$  and constant  $a$  from the polytropic analysis have become  $\lambda$  and  $b$  for the linear analysis to keep them distinct. This implies that

$$r = b\lambda. \quad (\text{B.22})$$

Once again we will make a change of variables

$$\rho = \alpha + \beta P \equiv \varrho \psi, \quad (\text{B.23})$$

where  $\varrho$  carries the dimensions of mass density and  $\psi$  is our new dimensionless parameter. We now differentiate this expression with respect to  $\lambda$  to produce

$$\frac{dP}{d\lambda} = \frac{\varrho}{\beta} \frac{d\psi}{d\lambda}. \quad (\text{B.24})$$

---

<sup>†</sup>In the language of Chapter 2,  $\alpha$  equals  $\rho_{CFL} - P_T/v_{CFL}^2$  and  $\beta$  equals  $1/v_{CFL}^2$ . We will use the notation  $\alpha$  and  $\beta$  for the remainder of § B.1.2 because it will simplify the form of the equations calculated.

Plugging Eqs. (B.23) and (B.24) into Eq. (B.21) produces an expression of the form

$$\frac{1}{\lambda^2} \frac{d}{d\lambda} \left( \frac{\lambda^2 d\psi}{\psi d\lambda} \right) = -\psi b^2 4\pi G \beta \varrho. \quad (\text{B.25})$$

By making a clever choice for the constant  $b$ ,

$$b^2 \equiv \frac{1}{4\pi G \beta \varrho}, \quad (\text{B.26})$$

we can eliminate the mess of constants on the right side of the last equation. Our final result

$$\frac{1}{\lambda^2} \frac{d}{d\lambda} \left( \frac{\lambda^2 d\psi}{\psi d\lambda} \right) = -\psi, \quad (\text{B.27})$$

is an equation very similar to the polytropic L-E equation.

Once again, we can modify this second-order equation to produce a system of coupled first-order equations. If we expand the derivatives, we get

$$\frac{d^2\psi}{d\lambda^2} - \frac{(\psi')^2}{\psi} + \frac{2}{\lambda}\psi' + \lambda^2 = 0. \quad (\text{B.28})$$

Defining and substituting the quantity

$$s \equiv \psi', \quad (\text{B.29})$$

we find

$$s' - \frac{s^2}{\lambda} + \frac{2}{\lambda}s + \lambda^2 = 0, \quad (\text{B.30})$$

where primes represent derivatives with respect to  $\lambda$ . Eqs. (B.29) and (B.30) are our system of first-order equations.

As with the polytrope, we need to set boundary conditions on  $\psi$  and  $s$ . These are straightforward to find, both in the center and at the surface of the neutron star. If we choose

$$\rho(r = 0) = \varrho, \quad (\text{B.31})$$

then Eq. (B.23) implies that

$$\psi(\lambda = 0) = 1. \quad (\text{B.32})$$

To derive the initial condition on  $s$ , we note from Eq. (B.24) that  $s$  is proportional to  $dP/dr$  at  $r=0$  because we can set  $\psi=1$  there. This implies that

$$s(\lambda = 0) = \lim_{\lambda \rightarrow 0} s = \lim_{r \rightarrow 0} \frac{dP}{dr}, \quad (\text{B.33})$$

which equals zero by Eq. (B.19):

$$s(\lambda = 0) = 0. \quad (\text{B.34})$$

As with the polytropic neutron star, the linear neutron star has  $P=0$  at its boundary with space. However, unlike the polytropic star, the linear star does not have  $\rho=0$  there. Instead,  $\rho$  at the boundary equals  $\alpha$ , as implied by Eq. (B.20).

### B.1.3 Hybrid

The hybrid equation of state is given by Eq. (2.8). In order to solve the equations of stellar structure with this equation of state, we will use the differential equations for  $\theta$  and  $\xi$  and for  $\psi$  and  $\lambda$  derived in the last two sections. We also need to define some quantities:  $r \equiv R$  is the surface of the star, while  $r \equiv R_T$  at the location where the quark transition occurs. This means that

$$r = \begin{cases} b\lambda, & r < R_T \\ a\xi, & r > R_T \end{cases}. \quad (\text{B.35})$$

Because we have already done all of the work of recasting the equations of stellar structure and the relevant equations of state into a useful form, the only thing to worry about now is how to join them at the transition radius. Given a central density, we start with the linear differential equations, Eqs. (B.29) and (B.30), and integrate them out until we reach the transition pressure  $P_T$ . After this point, we must solve the rest of the star with the polytropic differential equations, Eqs. (B.13) and (B.14)

until we find that  $P=0$ . Let's turn to figuring out what happens at the boundary.

First, we must match the parameters  $\lambda$  and  $\xi$  across the transition radius. Because both scale linearly with radius, the matching condition is straightforward:

$$\xi(r = R_T) = \frac{b}{a}\lambda(r = R_T). \quad (\text{B.36})$$

Furthermore, if we identify  $\mathcal{P}$  as the transition pressure  $P_T$ , then Eq. (B.7) gives the condition on  $\theta$  at the transition as

$$\theta(r = R_T) = 1. \quad (\text{B.37})$$

The last step is to find  $q$  at the transition radius. Both  $q$  and  $s$  are related to  $dP/dr$ , as can be seen from Eqs. (B.8) and (B.24):

$$\left. \frac{dP}{dr} \right|_{R_T+\epsilon} = \frac{\mathcal{P}(n+1)\theta^n}{a} \frac{d\theta}{d\xi}, \quad (\text{B.38})$$

and

$$\left. \frac{dP}{dr} \right|_{R_T-\epsilon} = \frac{v_{CFL}^2 \varrho}{b} \frac{d\xi}{d\lambda}. \quad (\text{B.39})$$

Because of the density discontinuity across the transition radius, Eq. (2.2) implies that  $dP/dr$  should also be discontinuous:

$$\frac{1}{\rho_{nuc}} \left. \frac{dP}{dr} \right|_{R_T+\epsilon} = \frac{1}{\rho_{CFL}} \left. \frac{dP}{dr} \right|_{R_T-\epsilon}. \quad (\text{B.40})$$

Combining these three equations and replacing  $\mathcal{P}$  with  $P_T$ ,  $\varrho$  with  $\rho_{central}$ , and  $\theta$  at the transition with 1 gives our last matching condition,

$$q(r = R_T) = \frac{\rho_{nuc}}{\rho_{CFL}} \frac{av_{CFL}^2}{b(n+1)} \frac{\rho_{central}}{P_T} s(r = R_T). \quad (\text{B.41})$$

## B.2 Implications

The Lane-Emden solutions presented above reveal an interesting relationship between the polytropic and linear equations of state. If we set  $\alpha$  equal to zero, the linear equation of state is simply the limiting case of the polytropic equation of state as  $n \rightarrow \infty$ . Because the exponent of a polytrope is a measure of how condensed a neutron star is, a linear neutron star seems to be nothing more than a very condensed polytrope. However, if we naively apply the results of § B.1.1 to the linear equation of state, we get nonsense. For example, if we let  $n$  go to infinity in Eq. (B.10), we find that  $a$ , and therefore the star's radius, approaches infinity, which is a bit distressing.

The solution to this dilemma turns out to be  $\alpha$ . It is indeed true that if we set  $\alpha$  equal to 0 for the linear equation of state, we get a star with infinite radius that matches the polytropic boundary condition of  $\rho=0$  at the surface. However, if  $\alpha$  is nonzero, we change this boundary condition such that  $\rho=\alpha$  at the surface. This has the effect of removing a portion from the outside of the star so that it ends at finite radius, the radius at which the density equals  $\alpha$ , which implies that  $\alpha$  must be nonzero for any physically correct linear model. Additionally, this means a neutron star with a linear equation of state has something resembling a solid surface, with  $\rho$  transitioning abruptly from a nonzero value to vacuum. This is very different from the behavior of a polytrope, whose mass density falls off to zero at its boundary with space gradually, like the atmosphere of a planet.





# Bibliography

- [1] L. D. Landau. Origin of stellar energy. *Nature*, 141:333, 1938.
- [2] F. Zwicky. On the theory and observation of highly collapsed stars. *Physical Review*, 55:726, 1939.
- [3] A. Hewish, S. Bell, J. Pilkington, P. Scott, and R. Collins. Observation of a rapidly pulsating radio source. *Nature*, 217:709, 1968.
- [4] Sean M. Carroll. *Spacetime and Geometry: An Introduction to General Relativity*. Addison Wesley, 2004.
- [5] Stuart L. Shapiro and Saul A. Teukolsky. *Black Holes, White Dwarfs, and Neutron Stars: The Physics of Compact Objects*. Wiley-Interscience, 1983.
- [6] Mark Alford, Krishna Rajagopal, Sanjay Reddy, and Frank Wilczek. Minimal color-flavor-locked–nuclear interface. *Phys. Rev. D*, 64:074017, 2001.
- [7] Robert C. Duncan and Christopher Thompson. Formation of very strongly magnetized neutron stars - Implications for gamma ray bursts. *Astrophysical Journal, Part 2 - Letters*, 392(1):L9–L13, 1992.
- [8] C. Kouveliotou, S. Dieters, T. Strohmayer, J. van Paradijs, G. J. Fishman, C. A. Meegan, K. Hurley, J. Kommers, I. Smith, D. Frail, and T. Murakami. An x-ray pulsar with a superstrong magnetic field in the soft gamma-ray repeater SGR 1806-20. *Nature*, 393:235–237, 1998.
- [9] Charles W. Misner, Kip S. Thorne, and John Archibald Wheeler. *Gravitation*. W. H. Freeman and Company, San Francisco, 1970.

- [10] Mark Alford and Sanjay Reddy. Compact stars with color superconducting quark matter. *Phys. Rev. D*, 67:074024, 2003.
- [11] Mark Alford. Private communication.
- [12] James B. Hartle and Kip S. Thorne. Slowly rotating relativistic stars. II. Models for neutron stars and supermassive stars. *The Astrophysical Journal*, 153:807–834, 1968.
- [13] James B. Hartle. Slowly rotating relativistic stars. I. Equations of structure. *The Astrophysical Journal*, 150:1005–1029, 1967.
- [14] Princeton pulsar catalog. <http://pulsar.princeton.edu/ftp/pub/catalog/>.
- [15] Deepto Chakrabarty. Private communication.
- [16] A. G. Lyne, M. Burgay, M. Kramer, A. Possenti, R. N. Manchester, F. Camilo, M. A. McLaughlin, R. D. Lorimer, N. D’Amico, B. C. Joshi, J. Reynolds, and P. C. C. Freire. A double-pulsar system: A rare laboratory for relativistic gravity and plasma physics. *Science*, 303(5661):1153–1157, February 2004.
- [17] J.L. Zdunik, P. Haensel, E. Gourgoulhon, and M. Bejger. Hyperon softening of the EOS of dense matter and the spin evolution of isolated neutron stars. *Astronomy and Astrophysics*, 416:1013–1022, 2004.
- [18] Paul Wiggins and Dong Lai. Tidal interactions between a fluid star and a Kerr black hole in circular orbit. *The Astrophysical Journal*, 532:530–539, 2000.